Hyperspectral Imaging Technology for Quality and Safety Evaluation of Horticultural Products: A Review and Celebration of the Past 20-Year Progress

Yuzhen Lu[1], Wouter Saeys[2*], Moon Kim[3], Yankun Peng[4] and Renfu Lu[1*]

[1] United States Department of Agriculture Agricultural Research Service, East Lansing, MI 48824, USA

[2] KU Leuven Department of Biosystems, MeBioS, Kasteelpark Arenberg 30, 3001, Leuven, Belgium

[3] United States Department of Agriculture Agricultural Research Service, Beltsville, MD 20705, USA

[4] College of Engineering, China Agricultural University, 17 Qinghua E. Rd., Haidian, Beijing, China

*Corresponding authors: wouter.saeys@kuleuven.be; renfu.lu@usda.gov

Abstract

In the past 20 years, hyperspectral imaging has been widely investigated as an emerging, promising technology for evaluating quality and safety of horticultural products. This technology has originated from remote sensing and joins the domains of machine vision and point spectroscopy to provide superior image segmentation for the detection of defects and contaminations, and to map the chemical composition. Thanks to the advancements in instrumentation and data analysis in the past two decades, hyperspectral imaging technology has evolved into a powerful nondestructive inspection tool and the scope of applications in postharvest quality and safety evaluation has expanded tremendously. In this article, different imaging modes (reflectance, transmittance, fluorescence and Raman) and their combinations, and the potential for real-time acquisition of hyperspectral images at industry relevant speeds are first discussed in terms of their advantages and disadvantages. Next reviewed are different data processing/analysis methods and associated steps from data pre-processing over the spectral and spatial domains to the actual model building and performance evaluation. An overview is then given of hyperspectral imaging applications for external quality and defect evaluation, internal quality and maturity assessment, and food safety detection of

horticultural products. Finally, a brief discussion is presented on the challenges and opportunities in future development and application of hyperspectral imaging technology in food quality and safety evaluation of horticultural products.

Keywords: Spectroscopy, imaging, fruit, vegetables, postharvest, quality, safety

1. Introduction

While the biological nature of horticultural products contributes to their high value as healthy sources of carbohydrates, vitamins and natural fibers, it also creates challenges with respect to the quality and safety assessment. Horticultural products are the result of a natural production process influenced by a wide range of factors such as genetics, environment, agronomic practices, etc. Moreover, horticultural products are not stable over time, but grow, mature, ripen and eventually perish as a result of metabolic processes during pre- and post-harvest periods. Consequently, their nutritional value, appearance and taste can vary widely between batches, and even within a batch. Hence, to ensure consumer satisfaction, the quality and safety of every product item should be inspected.

Appearance (i.e., color, size, shape and surface texture) can often be used as a proxy for product quality and safety, thanks to the interaction of light with the pigments and microstructure in horticultural products. Consequently, visual inspection is widely used throughout the horticultural production chain for rapid and non-destructive evaluation and sorting of the produce. While sorting based on visual inspection is still widely used in the horticultural sector, the limitations of human operators in terms of speed, volume and subjectivity, have inspired researchers to develop automatic sorting lines based on machine vision where the human eyes are replaced by a camera, the brain by a computer and the hands by an actuation system (e.g. ejector or tipping buckets). The first applications of machine vision made use of panchromatic cameras where each picture element (pixel) acquires a value which is proportional to the average intensity over a wide wavelength range (e.g. 400-1000 nm). This results in a greyscale image which allows to segment objects such as fruits, stalks and punctures based on image contrast. Early in the 1980's, Sarkar and Wolfe

(1985) already demonstrated this concept for tomato sorting. To increase the contrast between the relevant objects in the images, specific filters could be added in front of the camera to select a specific spectral portion.

Human (color) vision that is sensitive to red, green and blue light can be mimicked by different optical configurations (e.g., sequentially placing bandpass filters in front of a camera). An efficient way involves the deposition of a patterned filter on the camera chip consisting of squares. The most popular filter pattern, known as the Bayer filter, involves squares of 4 pixels with 1 blue, 1 red and 2 green filters to acquire RGB (red-green-blue) images. In the 1990's, RGB computer vision developed rapidly for quality grading and defect detection in the food industry (Brosnan and Sun, 2004) and on horticultural products such as apples (Throop et al., 1993) and tomatoes (Shearer and Payne, 1990). The significant increase in discriminating power provided by RGB imaging compared to panchromatic or monochromatic imaging inspired researchers to investigate the added value of utilizing more and other combinations of filters in the visible and near infrared (NIR) range. Imaging at multiple (typically 3-10) spectral bands is referred to as multi-spectral. For example, Mehl et al. (2002) showed the value of multispectral imaging for defect detection in apples, while Noordam et al. (2004) demonstrated its efficacy for inline defect and disease detection in the production of French fries.

In parallel with the investigations on computer vision for quality grading and sorting based on appearance, NIR spectroscopy, which covers the spectral region from 780 to 2500 nm that cannot be perceived by human eyes, was evaluated for rapid and non-destructive assessment of quality traits such as soluble solids content, titratable acidity and firmness (Nicolaï et al., 2007). In these studies, point measurements were performed in the visible (400-780 nm) and NIR (780 – 2500 nm) range with a spectral resolution of a few nm, providing spectral information at more than hundred wavebands, referred to as hyperspectral data. This allowed to obtain much more detailed information on the chemical composition of the samples. Early in the 1980's, researchers in remote sensing had already demonstrated the possibility to scan the earth surface with such a high spectral resolution, which gave birth to a new field known as imaging spectrometry or hyperspectral imaging (Goetz et al., 1985). The equipment for hyperspectral imaging used in remote sensing was extremely expensive. So, it took until the late 1990’s before this technology was introduced in food science (Gowen et al., 2007) and postharvest research (Lu and Chen, 1998; Martinsen and Schaare, 1998; Nicolaï et al., 2007) for more challenging classification tasks and mapping of the chemical composition, referred to as chemical imaging.

In this article, the progress in hyperspectral imaging technology for quality and safety evaluation of horticultural products since its introduction 20 years ago is reviewed. First, the instrumentation and imaging modes are discussed with special attention for the challenges related to real-time implementation. Then, the different steps in hyperspectral data analysis are discussed. Finally, an overview is given of hyperspectral imaging applications for external quality and defect evaluation, internal quality and maturity assessment, and food safety detection, followed by a brief discussion on challenges and future research needs.

2. Instrumentation and Imaging Modes

2.1. Overview

Instrumentation for hyperspectral imaging requires considering specific image acquisition approaches (i.e., point-scanning, line-scanning, area-scanning, and single shot or snapshot) and imaging or sensing modes (i.e., reflectance, transmittance, fluorescence and Raman), depending on the intended applications. Line and area scanning are widely used in hyperspectral imaging research for food quality inspection, and the former is well suited for inspecting food items moving along the production line. Snapshot or single shot is an emerging approach for hyperspectral image acquisition, which holds promise for real-time applications because of its fast imaging speed. Hyperspectral imaging can be implemented using one of the four sensing modes, or their combinations.

In any hyperspectral imaging system, there are three essential devices, i.e., light source, wavelength dispersive element and area-array detector (Lu et al., 2017). The light source can be a broadband quartz-tungsten-halogen (QTH), arc lamp, light emitting diodes (LEDs) or lasers. QTH lamps are most extensively used in hyperspectral imaging for food inspection, while narrowband LEDs and lasers are commonly used as an excitation light source in fluorescence and Raman imaging measurements. With the rapid developments in LED technology in recent years, broadband LED lighting is increasingly used for hyperspectral imaging. The wavelength dispersive element is usually composed of a diffraction grating based imaging spectrograph or an electrically tunable filter (ETF) [e.g., liquid-crystal tunable filter (LCTF) or acousto-optic tunable filter (AOTF)]. Different types of wavelength dispersive elements are associated with different image acquisition approaches. The imaging spectrograph is used for line scanning measurements, while the ETF is used for area scanning. For the area detector, there are multiple options available as well in terms of image sensor, such as charge-coupled device (CCD) or complementary metal-oxide-semiconductor (CMOS), and photo-sensitive elements: Silicon (Si), indium gallium arsenide (InGaAs) or mercury cadmium telluride (MCT). CCD represents the mainstream detectors for hyperspectral imaging, while CMOS is appealing and increasingly popular for real-time imaging applications. More detailed descriptions of these devices are given elsewhere (Lu et al., 2017; Qin, 2010).

Over the past two decades, both custom-assembled and commercial hyperspectral imaging systems have been used for food quality and safety evaluation. The former are built using modular components as described above, which are amenable to further modifications and improvements for meeting specific application needs, while the later come as all-in-one, ready-to-use hyperspectral imaging systems suitable for general applications.

2.2. Single Imaging Modes

The nature of light-matter interactions forms the foundation for optical imaging technologies like hyperspectral imaging. As schematically shown in Figure 1, the light incident on a turbid medium (e.g. a biological tissue) can be back-reflected after absorption and multiple scattering events, or via energy transfer between light and particles in the medium emitted in a different form of radiation such as fluorescence or Raman scattering, usually at longer wavelengths. However, it may also be transmitted through the medium without being fully absorbed. These light-matter interaction processes enable hyperspectral imaging to be implemented in reflectance, transmittance, fluorescence or Raman scattering mode by measuring respectively the reflected, transmitted or emitted light signals. Each of these imaging modes has different implications in quality and safety assessment of horticultural products (Lu et al., 2017; Qin et al., 2017a), and therefore will be described in detail.

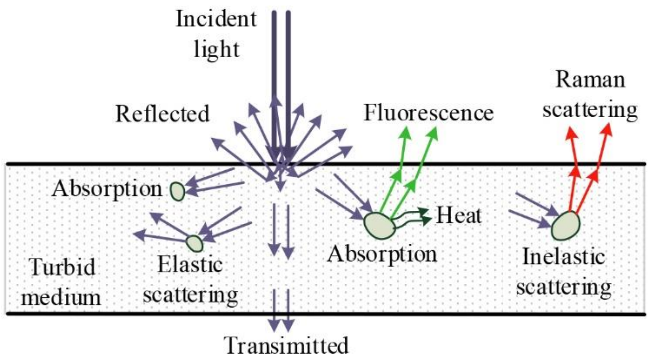

Figure 1. Schematic representation of light-matter interactions in a turbid medium illustrating four types of light that can be sensed in hyperspectral imaging, i.e., reflected, transmitted, fluorescence and Raman; the different color of the arrows for fluorescence and Raman scattering indicate that these photons have a different wavelength.

2.2.1. Reflectance

The standard configuration for reflectance imaging involves the use of diffuse light, as shown in Figure 2 (right). Diffusely or uniformly distributed light illuminates the sample, thus minimizing unwanted shadows or glares. This lighting mode is most extensively used in various machine vision applications for food product inspection (Cubero et al., 2011). Such diffuse light can be generated using a single line lamp or two line lamps symmetrically mounted around the object being imaged, as shown in Figure 2, or by mounting light sources within a hemispherical aluminum diffuser (Gómez-Sanchis et al., 2008a) or a lighting tunnel with an inner surface painted in white (Kleynen et al., 2005). As most horticultural produce is glossy and has a complex geometrical shape, it is recommended to optimize the positioning of the light sources based on ray tracing simulations (Keresztes et al., 2016b).

An alternative illumination mode involves point lighting with a narrow high-intensity light beam (e.g., ~1-2 mm in size), which can be generated by using point-like sources like lasers or focusing a broadband light beam, to interrogate biological samples. This creates a light scattering image at the surface of the sample, and by acquiring and analyzing scattering images from fruit samples, one could assess fruit texture (e.g., firmness, porosity) and flavor [e.g., soluble solids content (SSC)] (Lu, 2004; Lu, 2007; Lu and Peng, 2006; Wang et al., 2020). Moreover, based on light propagation models, the optical properties (i.e., absorption and scattering coefficients) of horticultural products can be estimated (Cen et al., 2012; Qin and Lu, 2008; Vanoli et al., 2020; Wang et al., 2020). Further information on this special variant of reflectance hyperspectral imaging and the methods to extract the optical properties from these measurements can be found in Lu et al. (2020) .

The diffuse reflectance imaging mode usually probes the superficial regions of biological samples within several millimeters below the sample surface, depending on imaging hardware setup and optical properties of the sample. Hence, this imaging mode is commonly used to detect surface or near-surface characteristics of horticultural products, such as surface defects (Mehl et al., 2004; Qin et al., 2009a; Zhang et al., 2015a), subsurface bruising (Lu, 2003; Lu and Lu, 2017a; Xing and De Baerdemaeker, 2005) and tissue decay (Gómez-Sanchis et al., 2008a; Li et al., 2016).

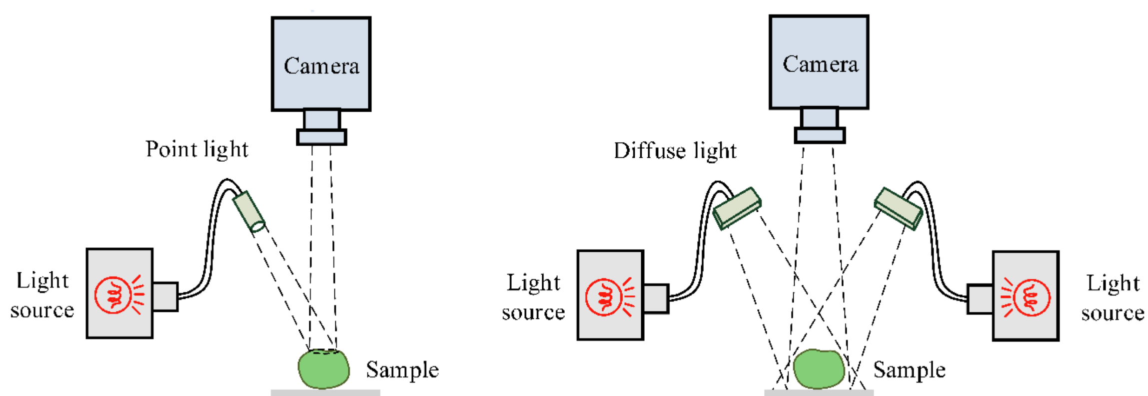

Figure 2. Schematic representation of reflectance imaging modes with point light (left) and diffuse illumination (right).

2.2.2. Transmittance

In transmittance imaging, as illustrated in Figure 3(left), the incident light and the camera are positioned on opposite sides of the sample with an angle of detection around 180°. Compared to reflectance imaging, such configuration is advantageous in detecting internal quality characteristics of samples, such as internal defects (Ariana and Lu, 2008a; Huang et al., 2013; Qin and Lu, 2005; Xing et al., 2008), given the fact that only light passing through the whole sample is measured. To yield detectable signals, transmittance imaging requires a high-intensity light source and a high-sensitivity detector (Ariana and Lu, 2008b). This makes it relatively costly and more difficult to implement in practice. Transmittance measurements may be influenced by product size and shape, since light attenuation within the product is dependent on the travelled light pathlength. Another issue is that clear-cut images cannot be readily obtained by transmittance imaging, because in most tissues the transmitted light has undergone many scattering events. In the reported applications on defect detection (Ariana and Lu, 2008a; Huang et al., 2013; Qin and Lu, 2005; Xing et al., 2008), (low-resolution) transmittance images were analyzed mostly for spectral features rather than defect visualization, which essentially reduces transmittance imaging to transmittance spectroscopy (Clark et al., 2003; Han et al., 2006).

As a compromise between diffuse reflectance and transmittance imaging, a semi-transmittance imaging mode has been suggested (Pan et al., 2017), where the light illumination area is separated from the imaging area by a specified distance or angle [Figure 3(right)]. This allows to acquire more information from the inside of the sample than the reflectance mode, because the measured light has gone through a minimal depth of tissue below the surface. This interactance imaging mode has been used in several studies (Pan et al., 2017; Wang et al., 2013).

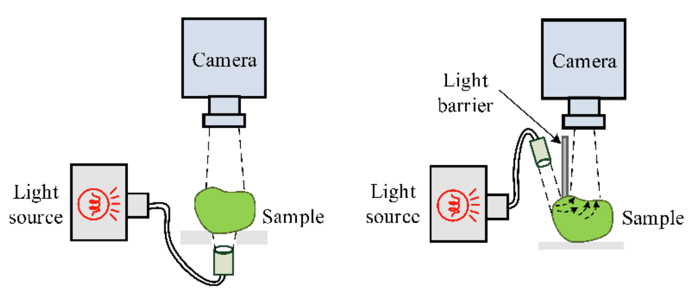

Figure 3. Schematic illustration of transmittance (left) and interactance (right) imaging modes.

2.2.3. Fluorescence

Biological materials, upon excitation by absorbing ultraviolet (UV) radiation or short-wavelength visible light, can emit longer-wavelength radiation. This phenomenon is known as fluorescence. Typical fluorescence spectra of plant materials are characterized by emission peaks in the blue, green, red and far-red regions, spanning a spectral range from 400 to 800 nm (Buschmann and Lichtenthaler, 1998). The blue and green fluorescence can be produced by cinnamic acids, while chlorophylls produce emission peaks in the red and far-red range (Buschmann et al., 2000). Imaging fluorescence emissions, especially at these four wavebands, provides a means for diagnosis of plant health conditions (Lichtenthaler and Miehe, 1997), and also for quality and safety inspection of horticultural products (Kim et al., 2002; Zhang et al., 2012).

In fluorescence imaging, the excitation light is critical for achieving high-yield fluorescence emissions. For example, radiation in the UV-A spectral region (long-wavelength UV in the 310-400 nm range) effectively excites the fluorophores in plant materials. Figure 4 shows two typical setups for hyperspectral fluorescence imaging. As in reflectance imaging, the light source and detector are generally positioned at the same side of the sample, and either broadband xenon arc lamps with high-intensity UV output or lasers or LEDs at appropriate wavelengths are used for sample excitation. In fluorescence imaging, it is important to control possible experimental artifacts due to ambient light or excitation light being detected. A simple technique illustrated in Figure 4(left) involves the installation of a shortpass filter (e.g., <400 nm) in front of the excitation light source and a longpass filter (e.g., >400 nm) in front of the camera (Kim et al., 2001b). Another way is to employ a time-gated detection system, in which a pulsed excitation light source (e.g., a short pulse laser) is used for excitation and the detection is electronically delayed relative to the excitation (Birlouez-Aragon et al., 2008). In addition, researchers have also used continuous-wave lasers coupled to a computer-controlled mechanical shutter, as shown in Figure 4(left), for fluorescence excitation (Noh and Lu, 2007). Under UV-A excitation, hyperspectral fluorescence images are typically captured in the 420-750 nm range, which covers the blue to far red region (Kim et al., 2001b; Kim et al., 2002). Like reflectance imaging, fluorescence imaging also probes superficial regions of samples and is mainly used to detect surface and near-surface characteristics. It is commonly used for food safety applications, such as detecting fecal contaminations and foreign materials (Kim et al., 2002; Mo et al., 2017a).

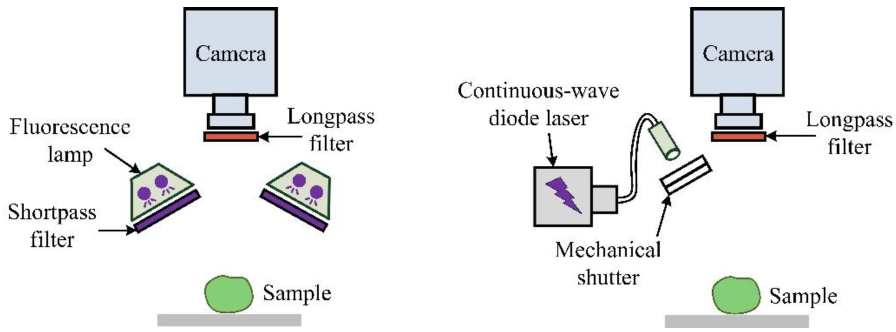

Figure 4. Schematic of fluorescence imaging using broadband lamps (right) and laser for excitation.

2.2.4. Raman

Hyperspectral Raman imaging, which is a two-dimensional (2-D) advancement over Raman spectroscopy that measures Raman scattering (Matousek and Morris, 2010), is a relatively recent technique for food quality and safety inspection. A hyperspectral Raman imaging system shares some similar requirements with the fluorescence imaging described above. Both Raman and fluorescence are weak (low-probability) processes (the former is even weaker), requiring an intense excitation light source and high-performance detector to ensure adequate signal quality. Moreover, they require blocking the excitation light from the detection end. For Raman measurements, an additional challenge is posed by the strong background of auto-fluorescence emission in many plant materials, which is generally several orders of magnitude stronger than the Raman signal. Such fluorescence interference needs to be eliminated or suppressed to avoid it from masking the Raman signal. To this end, the excitation is typically performed with diode lasers at 785 or 830 nm, because they generate less fluorescence than lasers at shorter wavelengths (Qin et al., 2016). A beam splitter at the excitation wavelength is preferentially used in Raman imaging to direct the incident light to the sample and resulting Raman-shifted light to the detector. As the Raman signals are very weak, commercial Raman imaging systems typically have small imaging areas at millimeter scales or less (for microscopic applications). Hence, there is a need to custom-design a macro-scale Raman imaging system for inspecting food items (Qin et al., 2010). Applications of hyperspectral Raman imaging have been reported on chemical mapping of horticultural products (Qin et al., 2011b; Qin et al., 2017b).

2.3. Integrated Imaging Modes

2.3.1. Integrated Reflectance and Transmittance

Integrated reflectance and transmittance imaging, compared to implementing them individually, has the advantage of simultaneous evaluation of external (e.g., color, size and surface defects) and internal (e.g., firmness, SSC and internal defects) quality characteristics of horticultural products. Ariana and Lu (2008b, 2008c, 2010) pioneered such reflectance-transmittance integrated hyperspectral imaging concept. It is well recognized that many biological tissues are almost opaque to visible light in the region of 400-675 nm because of strong light scattering and absorption, while red-NIR light in the region of 675-1000 nm has deeper tissue penetration. This motivated the development of the integrated reflectance and transmittance imaging system illustrated in Figure 5, in which the visible light was used for reflectance measurements to assess surface quality characteristics of samples, and the red-NIR light was used in transmittance imaging for internal quality assessment. The visible light was generated using a QTH lamp with light output filtered by a shortpass filter at the cut-off wavelength of 675 nm, and the red-NIR light was generated using a higher-power QTH lamp. Hyperspectral images covering the full wavelength range from 400 to 1000 nm were acquired using a single CCD camera. It should be noted that shortpass filters at other cut-off wavelengths (e.g., 700 nm) could also be used to lend measuring flexibility to the system. The integrated hyperspectral imaging system has demonstrated its effectiveness for the inspection of pickling cucumbers, whole pickles and blueberries (Ariana and Lu, 2008c, 2010; Leiva-Valenzuela et al., 2014; Lu and Ariana, 2013).

The broadband QTH lamps are inefficient, since the generated light above a cut-off wavelength is fully wasted and results in a considerable heat generation. Improvements were made to the above integrated imaging system by replacing the original QTH lamps with white LED lamps covering the 400-700 nm spectral region for reflectance imaging, and an NIR LED lighting module in the 700-1000 nm range for transmittance imaging (Cen et al., 2014). The use of white LEDs eliminates the need for a shortpass filter to de-mix reflectance and transmittance measurements.

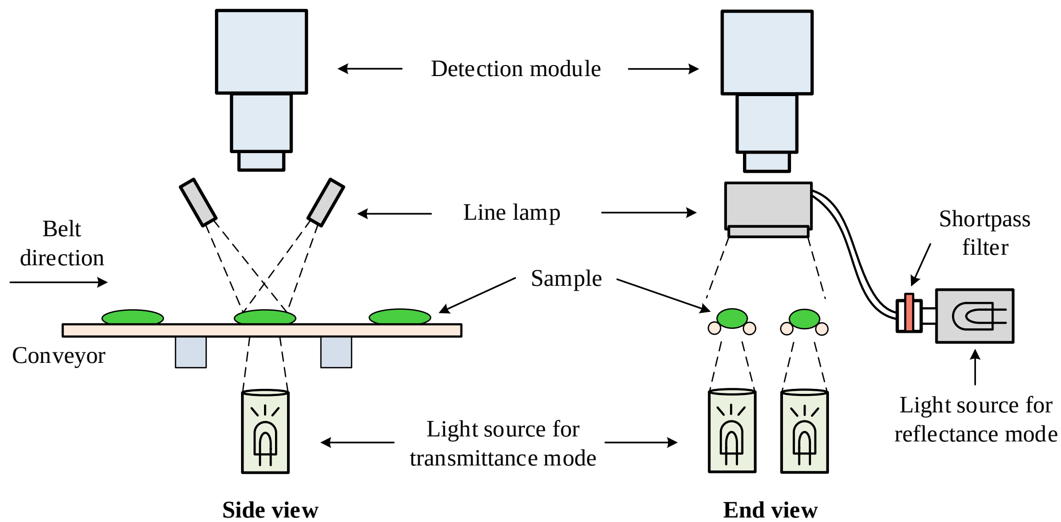

Figure 5. Schematic of an integrated hyperspectral reflectance and transmittance imaging prototype.

2.3.2. Integrated Reflectance and Fluorescence

Although both reflectance and fluorescence imaging are suited for detection of surface and subsurface characteristics of food commodities, they are based on different principles of light-matter interactions and may not be equally effective for specific applications. In general, reflectance imaging has a broader scope of applications, while fluorescence imaging was shown to be more sensitive for detecting some exogenous contaminants such as animal feces (Kim et al., 2001a; Kim et al., 2007) and certain stress-induced defects such as chilling or freezing damage (Slaughter et al., 2008). This suggests that the complementary use of both techniques may lead to a more versatile inspection tool.

Researchers at the U.S. Department of Agriculture Agricultural Research Service (USDA/ARS) in Beltsville, Maryland pioneered the technique of integrating reflectance and fluorescence imaging for food quality and safety assessment (Kim, 2015; Kim et al., 2007; Kim et al., 2001b; Kim et al., 2008; Lefcourt et al., 2006b). Figure 6 shows such an integrated hyperspectral imaging system in conjunction with a commercial fruit sorting machine, for the detection of fecal contamination and surface defects on apples using fluorescence and reflectance measurements, respectively. This system was equipped with an electronmultiplying CCD (EMCCD) camera, which is low-light sensitive, and two different light sources, a QTH lamp and a high-intensity UV-A lamp, enabling both fluorescence and reflectance measurements, respectively (Kim et al., 2007). A similar configuration integrating hyperspectral reflectance and fluorescence imaging, in which a diode laser at 408 nm was used for fluorescence excitation and a focused QTH light beam for reflectance measurement, was investigated for assessing apple maturity parameters (Noh et al., 2007). However, results for firmness, titratable acid and SSC prediction were relatively poor, compared to conventional point spectroscopy.

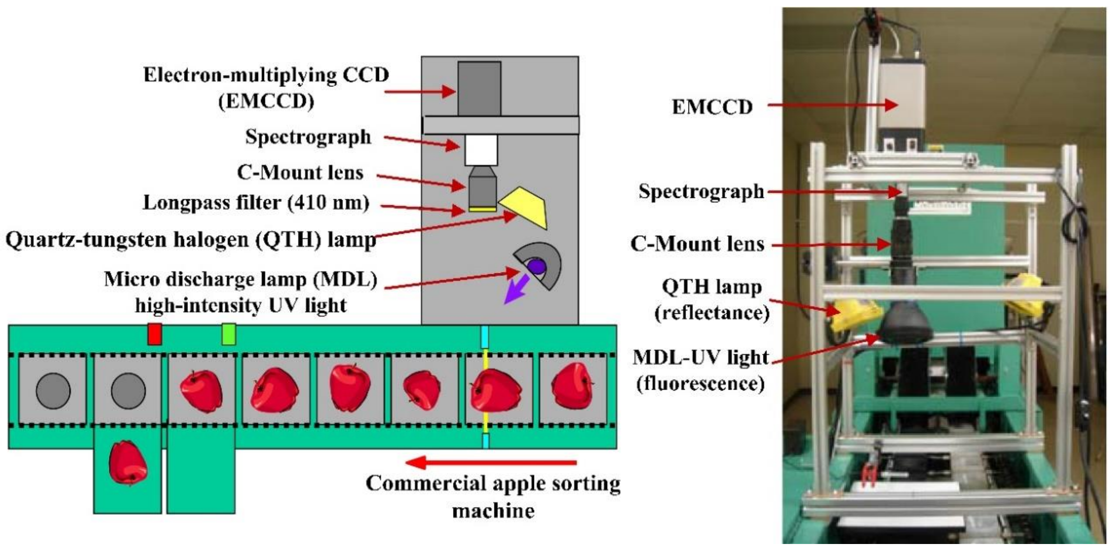

Figure 6. Schematic illustration (left) and photo (right) of an online hyperspectral reflectance and fluorescence line-scan imaging system. Reproduced with permission from Kim et al. (2007).

2.4. Real-time Imaging

Real-time hyperspectral imaging is faced with significant challenges, because of the need to acquire and process large volumes of image data at tens to hundreds of wavelengths. So far, the number of publications on real-time (full-spectrum) hyperspectral imaging for food quality and safety inspection is still limited. Keresztes et al. (2016a) implemented pixel-based early apple bruise detection using short-wave infrared (SWIR) hyperspectral imaging in real-time. However, the reported speed of 0.3 m/s was still short of meeting the industry needs. An alternative solution is to implement a line-scanning hyperspectral imaging system in multispectral mode, thus significantly reducing the workload of image acquisition and processing.

In addition, snapshot based hyperspectral imaging systems could provide opportunities for online application for quality and safety inspection of horticultural products. Several companies are now offering commercial systems for sorting seeds, nuts, fruit and vegetables in fresh, dried and processed form based on line-scan hyperspectral imaging mode (e.g. Insort Gmbh, Kirchberg an der Raab, Austria; TOMRA Systems ASA, Asker Municipality, Norway; Key Technology Inc., Walla Walla, WA, USA).

2.4.1. Line-scanning Mode

A line-scanning hyperspectral imaging system for real-time inspection needs dedicated hardware (e.g., efficient lighting, fast data acquisition and transfer devices, and powerful computers), well-decided working parameters (e.g. line-scanning spatial resolution and the number of wavelengths) and efficient software (e.g. image processing algorithms and implementations, and software architecture) (Park and Yoon, 2015). EMCCD is a low-light-sensitive camera that achieves fast image acquisition (<1 ms exposure times) and data transfer rates. An important feature of the EMCCDs is that they provide either contiguous or non-contiguous partial readout ability, which allows to readily implement a hyperspectral imaging system in a multispectral imaging mode at several discrete wavelengths. This hyperspectral-multispectral approach, pioneered by USDA/ARS researchers at Beltsville, Maryland, was used for inspecting apples for surface defects and fecal contaminants at a rate of 3-4 apples per second (Kim, 2015; Kim et al., 2007; Kim et al., 2008) and for inspecting poultry carcasses at an inspection rate of 140-180 birds/min for wholesomeness (Chao et al., 2007; Chao et al., 2010; Yang et al., 2009) and fecal contaminations (Park et al., 2011; Yoon et al., 2011). The technology for wholesomeness detection of broiler chickens (Chao et al., 2014; Chao et al., 2010) is now being commercialized, but its rate for fruit inspection still falls short of the industrial needs (e.g., 10 apples per second). Compared to poultry inspection, inspection of horticultural commodities, such as apples, is faced with two special challenges, i.e., whole surface inspection and reducing the false positives caused by the presence of stem and calyx tissues (Keresztes et al., 2017). The stem and calyx regions may be isolated based on the geometric features of products (Xing et al., 2007) or through supervised image segmentations (Unay and Gosselin, 2007).

2.4.2. Snapshot Mode

Snapshot or single shot imaging captures the entire three-dimensional (3-D) (x, y, λ) data cube through a single detector integration event, without scanning in either spatial or spectral domain. Compared to scanning based image acquisition, snapshot is advantageous in high optical throughput, lack of artifacts associated with scanning and increased compactness thanks to the absence of moving components. The technique thus offers a very promising solution to real-time imaging. However, the spatial and spectral resolutions for snapshot systems are typically lower compared to line-scanning systems.

There are a number of techniques that support snapshot spectral imaging, such as computed tomography imaging spectrometer, coded aperture snapshot spectral imager and image mapping spectrometry (Hagen and Kudenov, 2013). Recently, novel snapshot imagers based on pixel-level monolithic integration optical filters have become commercially available (Geelen et al., 2015; Geelen et al., 2013, 2014). These snapshot imagers enable fast hyperspectral measurements. For example, Geelen et al., (2015) acquired 170 datacubes of size 217×409×25 pixels per second in the region of 600-900 nm at lower spatial and spectral resolutions.

Snapshot hyperspectral imaging has been applied in the biomedical field (Kester et al., 2011; Pichette et al., 2016) and unmanned aerial vehicle based precision agriculture (Yue et al., 2017), but its application for horticultural product quality assessment is still at the infancy stage (Rungpichayapichet et al., 2017).

3. Hyperspectral Image Analysis

Hyperspectral image data are high-dimensional both spectrally and spatially. Therefore, both conventional methods that are commonly used in image and spectroscopic analysis and specific techniques that pertain to hyperspectral image data are needed in order to accomplish detection tasks. Basically, the raw hyperspectral data are sequentially subjected to five main treatment steps: data preprocessing, spectroscopic and image analysis, modelling and performance evaluation (Figure 7). In the context of machine learning for data analysis, all the data treatments prior to modeling can be loosely referred to as feature extraction. In the following subsections, only the principle or concept of these treatments is covered and the reader is referred to relevant literature for further details.

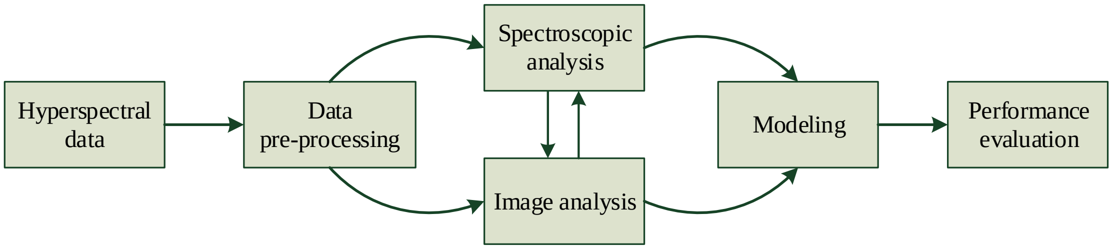

Figure 7. Flowchart of the main steps for hyperspectral image analysis.

3.1. Data Pre-processing

Data or image pre-processing involves radiometric correction, noise reduction and removal of other image artifacts related to illumination and spectral responses. Radiometric correction aims to correct for the variation in the spectral response of different detector units, like pixels in a CCD or CMOS area-array, and the non-flat geometry of samples. Flat-field corrections are most commonly used, in which reference and dark images are acquired and the corrections are done pixel by pixel for individual wavelengths (λ) according to the following equation:

$$I_{\text{corrected}}(\lambda) = \frac{I(\lambda) - I_{\text{dark}}(\lambda)}{I_{\text{standard}}(\lambda) - I_{\text{dark}}(\lambda)} \tag{1}$$

where I indicates the intensity value in a raw image, I_{dark} is the image acquired under dark environment (i.e. the light source is turned off and the camera lens is covered with an opaque cap), and I_{standard} is the image for a flat standard target. A flat Spectralon panel (Labsphere, Inc., Sutton, NH, USA), which has a uniform reflectance rate of 98% or higher for the entire visible and near-infrared region, is widely used for acquiring a reference image, although other types of reference panels may also be used. Fluorescence imaging, however, typically requires different targets that produce strong fluorescence emissions at corresponding wavelengths (Noh et al., 2007). For surface-curved samples, further geometric corrections for reflectance images may be required based on the actual 3-D geometry or surface contour of the samples (Gómez-Sanchis et al., 2008b; Peng and Lu, 2008).

Denoising is a routine practice for processing images acquired by an imaging system. Various filtering methods, in either spatial-domain or Fourier-domain, are widely used for noise reduction (Gonzalez and

Woods, 2008). Dimension reduction methods, like principal component analysis (PCA) (Saeys et al., 2019) and maximum noise fraction (MNF) (Green et al., 1988; Lee et al., 1990), also enable separation of the noise component. In addition, bi-dimensional empirical mode decomposition (BEMD) provides an adaptive data-driven method for noise removal, while also removing image vignetting (Lu and Lu, 2018b). Apart from noise, raw hyperspectral images may suffer from glares or dark spots resulting from the imperfection of imaging optics or the presence of abnormalities on the sample surface. These alter the intensities of the pixels at each waveband and consequently the spectral and spatial features in the images. These artifacts may be removed by applying a statistics filter (e.g., median filter) or image segmentation (Lange, 2005; Lu et al., 2017a).

3.2. Spectroscopic Analysis

Spectroscopic or spectral analysis deals with hyperspectral data in the spectral domain and prepares them for future multivariate modeling. It mainly includes spectral corrections and transformations, and dimensionality reduction. In addition to the aforementioned radiometric correction, spectral corrections, which are aimed at removing multiplicative scattering effects, baseline shifts and other unwanted systematic variations, are often needed, and they include multiplicative scatter correction (Isaksson and Næs, 1988), de-trending and standard normal variate transformation (Barens et al., 1989), and orthogonal signal correction (Westerhuis et al., 2001; Wold et al., 1998). These corrections may simplify the relationships between the spectra and the quality traits of interest and can thus improve the performance of the subsequent models. Data transformations, such as derivatives and logarithms, may also lead to improved spectral interpretability. For example, second-order derivatives are found to be effective in removing baseline shifts and enhancing spectral peak or valley positions. These corrections and transformations are commonly known as spectral preprocessing (Saeys et al., 2019; Varmuza and Filzmoser, 2009).

Dimensionality reduction, as a key step in the spectroscopic analysis, aims to reduce the number of dimensions of the spectral data. It simplifies data visualization, reduces computational cost, helps to identify or enhance useful spectral features, and improves model accuracy and reliability. There are two main types of dimension reduction methods: transformation and feature selection. The former reduces the dimensionality of the data through a transformation (e.g., moving and rotating), while retaining the information content as much as possible (van der Maatten et al., 2009). They include PCA, kernel PCA, independent component analysis (ICA), linear discriminant analysis (LDA), multivariate curve resolution (MCR), and so on. With PCA, which is by far the most popular dimension reduction method for spectral data, the original correlated spectral variables are replaced by a smaller number of uncorrelated linear combinations capturing the largest part of the variation in the data (Cowe and McNicol, 1985; Saeys et al., 2019).

Feature selection aims to select a number (much lower than the original dimension) of important features (i.e., wavelengths in the spectral analysis) relevant for the modeling tasks under study. Wavelength selection is essential for implementing hyperspectral imaging in a multispectral mode for online, real-time applications. There are three types of feature selection methods, i.e., filter, wrapper and embedded methods (Chandrashekar and Sahin, 2014; Saeys et al., 2007). The filter methods perform feature selection by thresholding on a certain measure based on the importance of variables [e.g., loading weights of principal components (PCs), correlation coefficient, mutual information, variable importance in projection (VIP) scores, etc.] derived from the dataset (the thresholding is sort of a filtering operation). This generally does not involve a learning algorithm. The features selected in this way may not be optimal for subsequent classification or regression purposes. The other two types of methods relate to specific learning algorithms. The wrapper methods use a search algorithm to find a subset of relevant features, and the model construction is wrapped within the search process. Since the model has to be trained for each subset of features, the wrapper methods are more computationally intensive than the filter methods. Examples of wrapper methods are sequential selection algorithms (Pudil et al., 1994) and partial least squares (PLS) based feature selection, such as uninformative variable elimination (UVE) (Centner et al., 1996), genetic algorithm (GA)-PLS (Leardi and González, 1998), competitive adaptive reweighted sampling (CARS) (Li et al., 2009) and interval partial least squares (Norgaard et al., 2000). The embedded methods embed the feature search process into the model construction, which may be more efficient than the wrapper methods. Random forest (RF) based (Díaz-Uriarte and de Andrés, 2006), neighborhood component feature selection (Yang et al.,

2012) and support vector machine (SVM) based feature selection algorithms (Guyon et al., 2002; Maldonado et al., 2011) are examples of wrapper methods. In addition, there are also other methods that combine (e.g. filter-wrapper), or even go beyond the scope of, the above methods. For more comprehensive reviews on feature selection methodologies the reader is referred to Chandrashekar and Sahin (2014) and Guyon and Elisseeff (2003).

3.3. Image Analysis

Image data play a crucial role in detecting spatial and morphological quality characteristics of horticultural products (e.g., size, shape and defects), as opposed to spectral data for chemical constituents. The goal of image analysis is to enhance, segment and extract image features pertaining to the quality characteristics of interest, which correspondingly requires image enhancement, image segmentation and texture analysis. In conventional machine vision, these methods are applied to the panchromatic or monochromatic images. While it is also possible to apply them to the individual images in a hyperspectral dataset, they are computationally intensive. Therefore, these methods are typically applied to a virtual image where the spectral data has been combined with one of the models discussed in Section 3.4 to obtain a chemical map or an image with maximal contrast.

Image enhancement provides an image with visually enhanced contrast and clarity. It can either be performed in the spatial or frequency domain linearly or nonlinearly. The spatial-domain linear methods are most commonly used, which include linear stretching, gamma transformation and histogram equalization (Gonzalez and Woods, 2008). These methods only stretch the global distribution of image intensities, which may not work well for specific tasks like edge detection. Spatial filtering, with a designed derivative filter mask is well suited for edge detection. A large family of unsharp masking operators based on emphasizing high-frequency information in the image provide another means for image enhancement (Ramponi et al., 1996). Many more advanced, often less efficient, methods rely on modifying the traditional histogram equalization method (Arici et al., 2009; Celik, 2012), because the shape of an image histogram provides a measure of image contrast. In addition, the BEMD method discussed above is also effective for image enhancement based on removing image noise and illumination vignetting (Lu and Lu, 2018b).

In most computer vision applications, image segmentation is a critical step to simplify higher-level vision tasks. For quality inspection of horticultural products, it involves two basic steps: background removal (i.e., extraction of the major objects such as fruit in the image) and segmentation of regions of interest (ROIs) (i.e., defects to be detected). If the image is captured under a well-controlled environment (e.g., in an enclosed dark chamber and with a clearly different background), simple thresholding techniques, in conjunction with morphological operations (e.g., filling and erosion), may suffice to remove the background from the image (Lu and Lu, 2017b). However, the second step normally requires more dedicated efforts, depending on the contrast of the ROI with its surroundings. In fruit defect detection, a large variety of morphological and textural properties for different types of defects complicate the accurate segmentation of these defects. For instance, surface russeting, which is a common web-like surface defect of fruits, is notoriously difficult to segment (Leemans and Destain, 2004). Apart from thresholding methods, other segmentation methods include edge-, region-, graph-, normalized cuts-, active contours, level sets, classification-based image segmentation, etc. (Sonka et al., 2015; Szeliski, 2011). These can be further categorized into unsupervised and supervised methods. Unsupervised methods are more straightforward to use, but computationally intensive and the outcome can vary considerably. On the other hand, supervised methods are typically more reliable and faster. However, they require manual labelling of the objects in a set of training images, which is tedious and prone to error. Semi-supervised segmentation strategies have been proposed to combine the advantages of both approaches (van Roy et al., 2017).

It should be noted that the difficult second-step image segmentation may be avoided in defect detection tasks. For example, in fruit sorting for defects, a suboptimal yet still acceptable solution is to eliminate defective fruit without providing specific information (e.g., location and shape) on the defects. So, only image-based classifications are needed, thus avoiding defect segmentation (Kavdir and Guyer, 2008; Lu and Lu, 2018a).

Apart from color and intensity differences, humans also largely rely on texture differences for detecting objects and shapes. Therefore, texture analysis has been proposed as an alternative method to identify objects and shapes in an image. Texture in an image can be quantitatively defined by a diversity of features that represent tonal and structural properties of the zones in an image (Haralick, 1979). Among the most extensively used features are the Haralick texture measures, statistical geometric features, local binary pattern (LBP), shape descriptors and statistical moments (Nixon and Aguado, 2012). In particular, LBP features (Ojala et al., 2002) have gained much attention in various classification tasks thanks to their superior performance. Essentially, a basic LBP is derived from a 3×3-pixel block by comparing the center pixel with its neighbors to yield an 8-bit binary pattern. This is then converted into a single decimal code for the center pixel. Finally, the LBP features are defined as the histogram of the codes for an entire image. Improvements have been made to the primitive LBP for achieving scale and rotation invariance (Ojala et al., 2002; Pietikainen et al., 2011). In addition, there are other well-known texture features or descriptors, e.g., Gabor-filter based features (Kamarainen et al., 2006), SIFT , HOG and SURF (Szeliski, 2011), just to name a few. One may use only one type of features or an ensemble of multiple types of features, with or without feature selection as described in Section 3.2, for model construction, which is discussed next.

3.4. Modeling

The goal of hyperspectral data analysis is to build a predictive or classification model. To exploit the high-dimensional nature of hyperspectral data, the model should be multivariate, and depending on specific detection tasks, it is either quantitative for providing numerical predictions (e.g. determining the concentration of chemical constituents), or qualitative to perform classifications (e.g. defect detection). Both types of models are constructed based on learning from the given data. Hence, separate data sets are required for training, validating (for model optimization) and testing the model (Marsland, 2015; Varmuza and Filzmoser, 2009; Saeys et al., 2019).

There are numerous multivariate techniques for quantitative modeling, mainly including multiple linear regression (MLR), principal component regression (PCR), partial least squares regression (PLSR), artificial neural networks (ANN), support vector regression (SVR), and kernel based learning methods (Scholkopf and Smola, 2002; Varmuza and Filzmoser, 2009; Saeys et al., 2019).

Developing qualitative models is the domain of pattern classification in machine learning (Hastie et al., 2009). The classification can be done by defining a linear (linear discriminant analysis – LDA) or quadratic

(quadratic discriminant analysis - QDA) discrimination function by combining the original variables. Alternatively, the classification of samples can be based on the class memberships of the samples which are most similar (closest) to the sample to be classified. This classification can then be done based on a majority vote (*k* nearest neighbors – k-NN) or a distance weighted function of the memberships (support vector machines - SVM, least squares support vector machines - LS-SVM and other kernel methods). As the spectral variables are typically highly correlated, it may be more interesting to define these functions based on the PC scores. Alternatively, the classifier can be based on disjoint PCA models for the different classes (soft independent modelling of class analogies - SIMCA). The regression methods, i.e., MLR, PCR and PLSR, can be also readily extended for classification purposes by coding dummy response variables for different classes and adopting a proper discrimination rule (e.g. LDA). A typical example of such an extension is PLS-discriminant analysis (PLS-DA).

Instead of combining the different variables in one discrimination function, a decision tree can be constructed by placing thresholds on the different variables to assign the samples to the different classes. Random forests, which is based on an ensemble of decision trees aided with a bootstrap aggregating sampling strategy (Breiman, 2001), is an emerging and increasingly popular classifier. Driven by technological advancements in computing capacity, deep neural networks (DNNs, as opposed to traditional shallower ANNs) or deep learning are becoming the workhorse for various large-scale machine learning tasks (LeCun et al., 2015). In particular, convolutional neural networks (CNNs) have enjoyed remarkable success in image classification and object detection, because they integrate feature extraction in the spectral and spatial domain with classification, and automatically learn low-level up to high-level abstractions from raw images.

The details of these methods and the guidelines to efficiently use these for multivariate calibration of spectral sensors for postharvest quality evaluation are beyond the scope of this article. Therefore, the interested reader is referred to the review paper on this topic which has recently been published in this journal (Saeys et al., 2019).

3.5. Performance Evaluation

Quantitative and qualitative models should be evaluated using performance metrics. For quantitative models, root-mean-square error (*RMSE*), standard error of prediction (*SEP*) and bias are the most frequently used metrics for the absolute error, while the coefficient of determination (R^2) is the most popular relative metric (Varmuza and Filzmoser, 2009; Saeys et al., 2019).

Qualitative models are usually evaluated against classification accuracy, which is defined as the number of correctly classified samples divided by the total number of samples, or the number of correctly classified samples for a specific class divided by the number of samples of that class. The accuracy calculated over all classes is the overall classification accuracy. However, only using the overall accuracy for model evaluation may create an accuracy paradox (i.e., a model with a high overall accuracy may have a low predictive power), since it gives no information on the classification performance for specific classes. Hence, apart from overall accuracy, it is highly recommended to provide the classification results for individual classes, such as false positive and false negative rates (or true positive and true negative rates). A confusion matrix gives a more complete and balanced evaluation of a model. In the special case of binary classification (i.e. discrimination between two classes), the metrics such as precision, recall, receiver operator characteristic curves (ROCs) as well as the overall accuracy are most commonly reported (Marsland, 2015). It should also be noted that in hyperspectral imaging, the classification level can be reported at the pixel level as well as at the object level. As the latter is typically what is most of interest from a practical point of view, it is highly recommended to evaluate the performance on that level.

4. Applications

The first applications of hyperspectral imaging for postharvest quality and safety inspection were reported in the late 1990s (Lu and Chen, 1998; Martinsen and Schaare, 1998). Thanks to the advancements in instrumentation and data analysis, hyperspectral imaging technology has evolved into a powerful nondestructive inspection tool and the scope of applications in postharvest quality and safety evaluation has expanded tremendously during the past 20 years and resulted in commercial applications on sorting machines. These applications mainly fall into three categories, i.e., external quality and defect evaluation, internal quality and maturity assessment, and food safety detection. This section gives a summary review of representative and updated research in these areas of applications.

4.1. External Quality and Defect Evaluation

The external quality of horticultural produce is evaluated for such attributes as size, shape, color, and the presence or absence of surface defects, which are among the most important factors in pricing horticultural products on the market. Size and shape can be readily evaluated using conventional machine vision, while color and defects, especially the latter, require a more effective modality like hyperspectral imaging. Defects can also occur beneath the surface or are hidden inside the products. Hyperspectral imaging in reflectance mode, in general, is limited to detecting surface defects or subsurface defects within a few mm of depth. While transmittance or interactance mode allows light to penetrate deeper into the tissues, it could not provide good quality images of internal tissue defects because the light detected by the hyperspectral imaging system has gone through multiple scattering events. Table 1 summarizes the major applications of hyperspectral imaging for color and defect evaluation.

Color is an important quality indicator for horticultural products, especially for perishable products like vegetables which require special efforts for color retention during postharvest handling. Hyperspectral imaging provides abundant, well-resolved spectral information and is thus well suitable for more precise color measurements than RGB imaging. Ariana and Lu (2008c) measured skin and flesh colors of pickling cucumbers using hyperspectral imaging in different imaging modes (i.e., reflectance, transmittance and their combination). Reflectance imaging mode was found to be the most effective for skin color measurement with R^2 values of 0.79 and 0.70 for chroma and hue, respectively. However, all three imaging modes resulted in poor flesh color measurements. In a later study, the authors reported on measuring surface color of pickles by directly integrating hyperspectral reflectance imaging data over the 500-675 nm range, instead of building predictive models (Ariana and Lu, 2010). In applying hyperspectral imaging to measure the color of vine tomatoes, van Roy et al. (2017) reported that the direct method, which is similar to the one used in Ariana and Lu (2010), performed poorly and was sensitive to intensity variation due to fruit curvature and glossiness, while multivariate modeling performed better. In addition to color measurements on intact products, hyperspectral imaging has been used for color-based quality inspection of fresh cut products, such as discriminating sound and discolored areas in fresh-cut lettuce (Mo et al., 2015).

Table 1. Applications of hyperspectral imaging for external quality and defect detection of horticultural products

Imaging mode	Applications		Reference
	Quality attribute	Product	
Reflectance	Color	Lettuce	Mo et al. (2015)
		Tomato	van Roy et al. (2017)
	Surface or visual defects	Apple	Lee et al. (2008); Mehl et al. (2002, 2004)
		Citrus	Li et al. (2011); Qin et al. (2008)
		Peach	Li et al. (2016); Liu et al. (2020); Zhang et al. (2015a)
		Hazelnuts	Moscetti et al. (2015)
	Physiological disorders	Apple	ElMasry et al. (2009); Huang and Lu (2010); Li et al. (2019); Nicolaï et al. (2006)
		Cucumber	Cheng et al. (2004); Liu et al. (2005)
		Peach	Liu et al., (2020); Pan et al. (2016)
	Subsurface bruising	Apple	Baranowski et al. (2013); ElMasry et al. (2008); Keresztes et al. (2016b); Lu et al. (1999); Lu (2003); Xing et al. (2005); Xing and De Baerdemaeker (2005); Xing et al. (2007)
		Mushroom	Gowen et al. (2008)
		Potato	Lopez-Maestresalas et al. (2016)
		Strawberry	Nagata et al. (2006)
Transmittance	Internal defects	Blueberry	Zhang et al. (2017); Zhang et al. (2020)

		Cherry	Qin and Lu (2005); Siedliska et al. (2017)
		Cucumber	Ariana and Lu (2010)
		Nectarine	Munera et al. (2019)
		White radish	Pan et al. (2017); Song et al. (2016)
Reflectance and Transmittance	Physiological disorders	Cucumber	Cen et al. (2016)
	Internal defects and color	Cucumber	Ariana and Lu (2008c; 2010); Cen et al. (2014)
Reflectance and fluorescence	Surface defects	Apple	Ariana et al. (2006)

Defect detection in horticultural products is challenging, because there exist large variations in morphological and/or physiological characteristics of defects (Lu and Lu, 2017c). Hyperspectral imaging has been reported for detecting a range of defects, either surface, subsurface or internal by implementation of an appropriate imaging mode. For the convenience of discussion, defects of horticultural products are loosely categorized into four types: surface or visual defects (i.e., the defects occurring on the surface of products or defects that are externally visible), physiological disorders (i.e., those well-identified defects due to physiological stress, such as bitter pit and chilling injury), subsurface bruising, and internal defects. Except surface or visual defects, other types of defects may be barely visible or totally invisible to the human, depending on the severity of the defect.

Mehl et al. (2002) were among the first to apply hyperspectral imaging for **surface defect detection** in fruits. In detecting surface defects on apples, they identified three effective wavebands 460, 575 and 705 nm based on PCA of hyperspectral images. These bands were implemented in a multispectral imaging system and resulted in overall detection accuracies of 76-95% for three apple varieties. Later on, they proposed an asymmetric second difference method for processing hyperspectral images to enhance defect detection in apples (Mehl et al., 2004). Lee et al. (2008) presented a correlation analysis (CA) method based on two-wavelength image ratios or differences for identifying the best pairs of wavebands for surface defect detection in apples. The two-wavelength image ratio R670 /R684 nm (R denotes reflectance) was the most effective for defect detection with a 92% detection rate. This method, however, requires an exhaustive search for all possible two-wavelength pairs. Qin et al. (2011a) applied the CA method for detecting citrus canker (surface defect caused by diseases) by hyperspectral imaging and identified the best wavelength ratio R834/R729 nm, which achieved an overall detection accuracy of 95%. Using high-dynamic range hyperspectral reflectance imaging in the SWIR (1000-2500 nm) region, Moscetti et al. (2015) classified hazelnuts (cv. Tonda Gentile Romana) in four quality classes commonly used in industry: i.e., the presence/absence of discolorations, infestations, infections and/or detrimental disorders. After the spectral pretreatment optimization, the multi-class PLS-DA classifier provided good (>80%) to very good (>90%) sensitivity and selectivity.

Horticultural products are prone to numerous **physiological disorders** which develop mostly post-harvest due to internal or external stresses such as extreme temperature, nutritional deficiency, senescence and suppressed respiration. Chilling injury (CI) is a serious physiological disorder during postharvest handling of horticultural commodities of tropic or subtopic origin like cucumbers, apples and peaches. Cheng et al. (2004) reported on using hyperspectral imaging for CI detection in cucumbers. Combination of PCA-LDA as a hybrid dimension reduction technique with k-NN for classification achieved detection rates of 91-93% for CI cucumbers (Cheng et al., 2004). Later, Liu et al. (2006) compared two methods, i.e., a simple dual-waveband ratio R811/R756 nm and PCA-SIMCA for CI detection of cucumbers and reported comparable detection rates over 90%. Early CI detection is difficult, because of the absence of visible symptoms. Cen et al. (2016) applied hyperspectral reflectance and transmittance imaging for detecting CI in pickling cucumbers. They compared different classifiers combined with feature extraction and selection techniques for classifying cucumbers, achieving the best overall accuracies of 92% and 100% for three-class and two-class classification schemes, respectively. Hyperspectral imaging has also been used for detecting CI in other horticultural products such as apples (ElMasry et al., 2009) and peaches (Pan et al., 2016).

Bitter pit is a calcium deficiency-induced physiological disorder in apples, which is usually initiated pre-harvest, but progresses rapidly during postharvest storage. The defect mainly occurs under the epidermis and is not externally visible. Nicolai et al. (2006) first reported on using hyperspectral reflectance imaging combined with PLS-DA based pixel-level classification for bitter pit detection (Nicolaï et al., 2006). The model enabled identifying bitter pit lesions before visual symptoms had developed, as shown in Figure 8, but it could not discriminate these from the corky tissues (e.g., the defective but non-bitter pit lesion occurring in the image center in Figure 8).

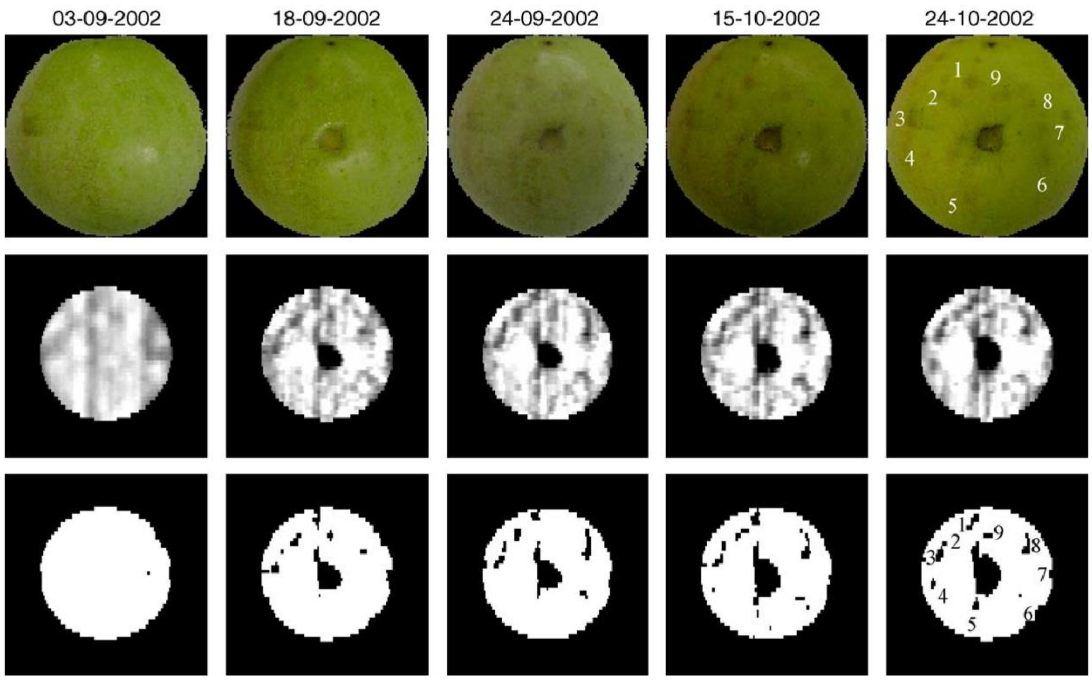

Figure 8. Development of bitter pit during storage: digital images (top row); predicted images based on modelling (middle row) and binary images showing bitter pit lesions (bottom) row. The numbers in the right most images indicate bitter pit lesions. Reproduced with permission from Nicolaï et al. (2006).

Improper postharvest handling operations would subject horticultural products to excessive impact, compression or vibration forces, which could cause bruising to the products, thus lowering the quality grade and resulting in revenue loss. The bruised tissues are situated beneath the surface of the products with barely visible symptoms, which is referred to as subsurface bruising. Bruises can also appear deep inside the products, which is referred to as internal bruising. There has been continued interest in developing effective techniques such as hyperspectral imaging for subsurface bruising detection in fruits. Lu et al. (1999) first reported on bruise detection in apples by hyperspectral reflectance imaging. PCA transformation of the hyperspectral images in the 700-900 nm wavelength range enabled identifying all the newly generated bruises as well as most pre-existing ones (Lu et al., 1999). Later, Lu (2003) found that the spectral region of 1000-1340 nm was also informative for bruise detection and achieved detection rates of 62-88% for 'Delicious' and 59-94% for 'Golden Delicious' apples between 0 and 47 days after bruising (Lu, 2003). Studies were also reported on detection of bruises of at least 1-day old with hyperspectral imaging in the 400-1000 nm range for 'Jonagold' and 'Golden Delicious' apples (Xing and De Baerdemaeker, 2005; Xing et al., 2005). An ideal detection system should be able to detect both new and old bruises. ElMasry et al. (2008) investigated bruise detection for 'McIntosh' apples over a period of 1 h to 3 days after bruising, using three wavelengths of 750, 820 and 960 nm selected based on VIP scores from PLS analysis, along with adaptive thresholding. Recent studies demonstrated the feasibility of real-time bruise detection in apples by hyperspectral imaging in the SWIR range (1000-2500 nm) at conveyor speeds up to 0.3 m/s and with a prediction accuracy of 98% (Keresztes et al., 2016a). Hyperspectral imaging has also been investigated for bruise detection in mushrooms (Gowen et al., 2008), potatoes (Lopez-Maestresalas et al., 2016) and strawberries (Nagata et al., 2006). More studies on bruise detection by hyperspectral imaging are listed in Table 1.

Internal defects are hidden inside biological tissues and are more difficult to detect than surface and subsurface defects. This would require performing transmittance measurements for interrogating deeper tissues. Cucumbers, after being subjected to excessive mechanical stress, can be internally bruised, leading to carpel separation and even hollow center. Ariana and Lu (2008a) first applied hyperspectral transmittance imaging for detecting internal mechanical injuries in pickling cucumbers (Ariana and Lu, 2008a). They reported that the NIR wavelength region of 700-1000 nm had much higher transmittance and was thus more effective for internal injury detection than the visible range of 450-700 nm. PLS-DA models achieved classification accuracies of 90% and 99% based on mean spectra and 89% and 95% for the pixel-based spectra for two varieties of cucumbers. In subsequent research, a laboratory online imaging system integrating transmittance for the NIR range and reflectance for the visible range was developed and used for simultaneous detection of both external quality and internal injury of cucumbers (Ariana and Lu, 2008b, 2008c and Figure 5). Hyperspectral transmittance and/or reflectance imaging has also been used for detecting other internal defects such as pits in cherries (Qin and Lu, 2005; Siedliska et al., 2017), blackheart in white radish (Song et al., 2016), and internal injuries in blueberries (Throop et al., 1993; Zhang et al., 2017).

4.2. Internal Quality and Maturity Assessment

Internal quality discussed here is referred to as texture, flavor and nutritional value, which cannot be readily detected through visual inspection. These quality features would normally require destructive physicochemical analysis (e.g., the Magness-Taylor test for firmness and the Brix refractometer for SSC measurement). Firmness is the primary textural attribute of horticultural products, and the sensory properties such as sweetness, sourness and bitterness, in conjunction with various volatile compounds, form the characteristic flavor. Nutrients include vitamins, minerals, fibers, antioxidants, etc. in the products (Golding and Wills, 2016). Evaluation of internal quality has been a key theme in non-destructive quality assessment of horticultural products.

Based on light scattering principles, an innovative hyperspectral scattering imaging technique was developed for assessing internal quality of fruits (Lu, 2007; Lu and Peng, 2006; Vanoli et al., 2020; Wang et al., 2020). This technique, which is based on the relation between light scattering and structured and textural properties of biological tissues, uses a highly focused light beam to generate scattering images as described in Section 2.2.1, so as to enhance assessment of fruit firmness. In using hyperspectral scattering for measuring firmness of peaches, Lu and Peng (2006) built firmness prediction models by applying step-wise MLR to the parameters of scattering profiles, achieving R^2=0.77 and 0.58 for 'Red Haven' and 'Coral Star's peaches, respectively. A detailed description of the analysis of hyperspectral scatter images and characterization of scattering profiles for fruit quality assessment is given in Lu et al. (2017). In a later study, Lu (2007) applied hyperspectral scattering imaging coupled with ANN models to assess firmness and SSC for apples, which resulted in firmness predictions of R^2 = 0.76 and 0.55 and better SSC predictions of R^2 = 0.79 and 0.64 for 'Golden Delicious' and 'Delicious' apples, respectively. It was hypothesized that the relatively poor predictions for ‘Delicious’ might be attributed to the more irregular fruit shape, which could have negatively affected the scattering measurements. Relatively poor predictions of SSC, compared to point Vis/NIR spectroscopy, could be attributed to the lower signal to noise ratio and the fact that light scattering technique tends to enhance structural features which would be more conducive to firmness prediction than SSC prediction.

Apart from light scattering and spectral characteristics, image textural features, which carry information on the structural or morphological properties of samples, can also be useful for quality evaluation. Mendoza et al (2011) integrated hyperspectral scattering profile and image textural features for measuring firmness and SSC of apples. This led to significantly improved predictions. An attempt to integrate hyperspectral image data with those obtained by other sensing techniques such as NIRS also resulted in improved prediction accuracies (Mendoza et al., 2012). However, the use of multiple sensing techniques for postharvest quality evaluation may not be practically viable at present, because of the increased complexity and instrumental costs. Mendoza et al. (2014) further applied hyperspectral scattering imaging to grade apples for firmness and SSC. Two-grade grading accuracies of 78-98% for firmness and 62-92% for SSC were attained at an image acquisition speed of 0.5 fruit/second. It should be noted that the grading was performed through offline analysis.

In addition to hyperspectral scattering techniques, LCTF-based hyperspectral reflectance imaging in the 450-650 nm range under wide-field illumination rather than focused point light, was used for measuring firmness and SSC in strawberries (Nagata et al., 2004). Tallada et al. (2006) further tested an NIR hyperspectral imaging system for firmness prediction of strawberries and identified three effective wavelengths (685, 865 and 985 nm). ElMasry et al. (2007) also reported on the assessment of strawberry internal quality. Using MLR for selected wavelengths, the authors achieved prediction accuracies of R^2= 0.76, 0.64, and 0.85, and SEP = 5.8%, 0.21% and 0.09 for moisture content (MC), SSC and pH, respectively. More applications of hyperspectral reflectance imaging for internal quality assessment for a diversity of horticultural products are listed in Table 2. In addition, hyperspectral imaging in fluorescence (Noh and Lu, 2007) and integrated reflectance and transmittance imaging mode (Leiva-Valenzuela et al., 2014; Noh et al., 2007) have also been utilized for assessing apple and blueberry quality. However, they often did not lead to improved accuracies compared to reflectance imaging (Leiva-Valenzuela et al., 2014). Despite the progress made so far, hyperspectral imaging has not yet been implemented for real-time fruit grading based on internal quality traits such as firmness and SSC, while point spectroscopy has been implemented for the latter.

Table 2. Applications of hyperspectral imaging for internal quality and maturity evaluation of horticultural products

Imaging mode	Application		Reference
	Quality attribute	Product	
Reflectance	Maturity or shelf life	Apple	Menesatti et al. (2008); Peirs et al. (2003)
		Banana	Rajkumar et al.(2012)
		Blueberry	Yang et al. (2014)
		Mango	Wendel et al. (2018)
		Mushroom	Taghizadeh et al. (2010)
		Peach	Lleó et al. (2011)
		Pear	Khodabakhshian and Emadi. (2018)
		Tomato	Polder et al. (2004)
	Texture and flavor	Apple	Lu (2007); Mendoza at al. (2011, 2012, 2014); Ma et al. (2018); Peng and Lu (2008); Qin et al. (2009b)
		Blueberry	Leiva-Valenzuela et al. (2013)
		Grape	Fernandes et al. (2011)
		Kiwifruit	Guo et al. (2015)
		Pear	Fan et al. (2015); Yu et al. (2018)
		Persimmon	Munera et al. (2017)
		Plum	Li et al. (2018)

		Strawberry	ElMasry et al. (2007); Nagata et al. (2006)
Fluorescence	Texture and flavor	Apple	Noh and Lu (2007)
Raman	Maturity	Tomato	Qin et al. (2011b)
Reflectance and transmittance	Texture and flavor	Blueberry	Leiva-Valenzuela et al. (2014)

In determining internal quality attributes, it is not uncommon to average the spectra of pixels within an ROI to reduce the hyperspectral datacube for a sample into a single spectrum, followed by multivariate modeling and quality prediction. However, this approach does not take advantage of the capability of hyperspectral imaging for mapping or visualizing the spatial heterogeneities within the produce. Hyperspectral imaging can be used for generating a map of the quality attribute distribution of the sample at the pixel level. Martinsen and Schaare (1998) were the first to utilize hyperspectral imaging for mapping postharvest quality attributes. To measure the SSC distribution over the cut section of kiwifruit, they built separate predictive models for the core and pericarp fruit tissues. Polder et al. (2004) reported on using hyperspectral imaging for measuring the distribution of carotenes (including lycopene, lutein and β-carotene) and chlorophylls in ripening tomatoes. Pixel-level predictive models were built by randomly selecting 200 pixels per sample. It was noted that pixel-level modeling requires dense sampling points to obtain ground-truth reference values and also lengthy model calibration processes. The lycopene distribution in tomatoes was also mapped using hyperspectral Raman imaging (Qin et al., 2011b). Rungpichayapichet et al. (2017) recently used a snapshot hyperspectral camera for mapping the quality attributes of mangoes. The prediction maps for firmness, total soluble solids (TSS) and titratable acidity (TA) obtained for mangoes at different ripening stages are illustrated in Figure 9. These clearly reveal quality attribute changes during fruit ripening and their heterogeneity within individual fruits. However, it should be noted that the values close to the edge of the fruit are very different from those in the center. This might be attributed to effects of the fruit curvature on the acquired spectra. To verify this hypothesis, the locally predicted values should be verified against ground truth values for densely sampled points, as proposed by Polder et al. (2004).

Maturity assessment is important for determining harvest timing and to optimize postharvest options and storage regimes. Multiple parameters are often used for maturity assessment, which include color, firmness, starch pattern index, SSC, acid and ethylene (Reid, 2002). Polder et al. (2002) first reported on using hyperspectral imaging for assessing maturity of tomatoes. Hyperspectral imaging in the visible range of 396-736 nm was found to be superior to traditional color imaging in classifying tomatoes into five ripeness stages based on LDA models. The maturation of apples is commonly characterized by the degree of degradation of starch into sugars, which is routinely determined through starch-iodine tests. Peirs et al. (2003) first applied hyperspectral imaging as an alternative to the standard starch-iodine test to determine the starch index of apples. The PC-1 score images extracted from the hyperspectral images revealed a pattern of starch breakdown during fruit maturation, which correlated well to that obtained with the conventional iodine test. Menesatti et al. (2009) extended the starch index evaluation by applying supervised pixel-based classification on hyperspectral images. The color images of iodine test results for apples of various maturity stages were segmented into two regions (i.e. starch and starch-free) by a *k*-NN model, serving as ground-truth starch index levels. Afterwards, PLS-DA models were built to classify each pixel into starch-free and starch classes. Classification accuracies of 81% and 66% were obtained by two types of PLS-DA models that were built for each fruit sample and all samples together, respectively. It should be noted that both studies on starch index evaluation required destructive sampling. Lleó et al. (2011) proposed optical indices for rapid assessment of peach maturity, which were derived from the reflectance ratios at three selected wavelengths (640, 680 and 730 nm) around the chlorophyll absorption peak (Lleó et al., 2011). The index [R680/(R640+R730)], which was focused on the shape of the chlorophyll absorption, was found to be the most discriminative between ripening and non-ripening stages.

All the above studies on maturity assessment were aimed towards postharvest quality inspection. In-field or pre-harvest maturity assessment would be beneficial for yield estimation and deciding on the harvest date. Yang et al. (2014) reported on in-field maturity assessment of blueberries by hyperspectral imaging under natural lighting conditions. In classifying three maturity stages of fruit plus background, classification accuracies of 88% and higher were achieved using different pattern classifiers coupled with wavelength selection. More recently, Wendel et al. (2018) were the first to report on orchard-scale maturity mapping of mangoes based on predicting dry matter (DM) content using a mobile hyperspectral imaging platform. Ground-truth DM values were measured with a hand-held NIR spectrometer. For hyperspectral imaging, fruit pixels were first segmented based on pixel-level classifications, after which multivariate models were built for DM prediction for each pixel, which resulted in the best cross-validation accuracies of R^2 =0.64 and RMSE = 1.08% w/w for fruit on trees. Further, the predicted DM values were projected to a world coordinate system, leading to maturity mapping on an orchard scale.

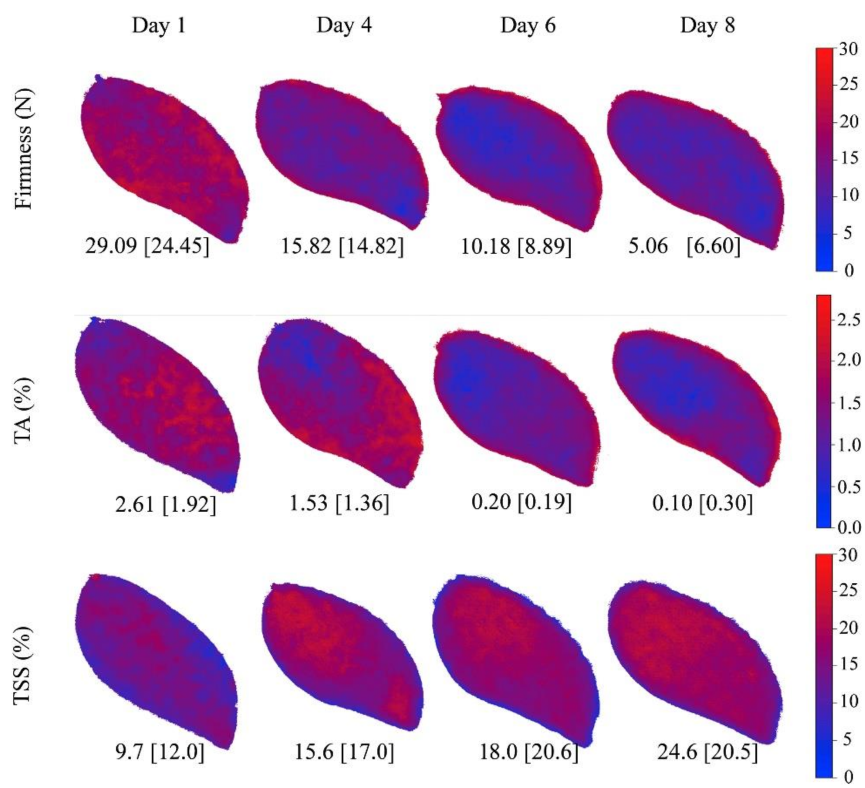

Figure 9. Prediction maps showing the distribution of firmness, titratable acidity (TA) and total soluble solids (TSS) for 12 mango samples during ripening with measured and predicted (in brackets) quality attribute values. Reproduced with permission from Rungpichayapichet et al. (2017).

4.3. Food Safety Inspection

The food safety factors discussed here include fecal contamination, defects caused by microbial (bacterial and fungal) infection, insect or pest infestation, and pesticide residues. These defects can be collectively seen as biological contamination. These concerns, which are closely related to food-borne diseases, represent more severe quality issues than those described above and are normally inspected against more stringent standards. Fresh produce should be free from these safety issues, and any bulk lot containing those unsafe products is likely to be inspected against a stricter tolerance (e.g., 1% ppm level or even zero tolerance) to meet the grading requirements. Hence, there is a strong incentive to develop potent nondestructive technologies such as hyperspectral imaging for food safety inspection.

Researchers with the USDA/ARS at Beltsville, Maryland did extensive research on using hyperspectral fluorescence imaging for detection of fecal contamination on fresh produce (Kim, 2015; Kim et al., 2001a; Kim et al., 2001b; Kim et al., 2004; Kim et al., 2002). Fecal matters from cattle, swine, deer and other animals are the common sources of fecal contamination. They emit fluorescence upon excitation with UV radiation, making fluorescence imaging a suitable modality for fecal contamination detection. In detecting fecal contamination on apple surfaces, Kim et al. (2002) used PCA to identify four effective wavebands around 450, 530, 685 and 735 nm, which corresponded to four fluorescence emission peaks in the blue, green, red and far-red regions, respectively. These wavebands can be used for rapid multispectral imaging (Kim et al., 2005; Lefcourt et al., 2003) and also enable image fusion or ratio analysis for enhanced detection. The waveband ratio images, in particular, greatly reduce the variation due to the fruit surface colorations, while accentuating image contrast, facilitating segregation of the contaminated spots based on simple thresholding (Kim et al., 2004; Kim et al., 2005). Using single-band images and two-band ratio images, Lefcourt et al. (2003) reported that the 1:2 and 1:20 dilutions of animal feces, which were artificially applied on the surfaces of apples, were detected with accuracies of nearly 100%, and that the detection accuracy for 1:200 dilutions diminished, but still exceeded 80%. Other methods that enhanced the detection of fecal contamination on apples include two-band differences and universal power transformation (Lefcourt and Kim, 2006). Reflectance imaging has also been used for fecal contamination detection, but it was much less sensitive than fluorescence imaging for detecting highly diluted (e.g., 1:200) or thin fecal smear spots (Lefcourt et al., 2006; Liu et al., 2007). Table 3 summarizes some important works on fecal contamination detection on horticultural products.

Table 3. Applications of hyperspectral imaging for food safety detection of horticultural products

Imaging mode	Application		Reference
	Safety attribute	Product	
Reflectance	Fecal contamination	Apple	Kim et al. (2001a)
	Microbial infection	Apple	Pieczywek et al. (2018)
		Citrus	Gómez-Sanchis et al. (2008a, 2008b, 2013, 2014); Li et al. (2016)
		Spinach	Siripatrawan et al. (2011)
	Insect infestation	Apple	Rady et al. (2017)
		Jujube	Wang et al (2011)
		Mango	Haff et al. (2013); Saranwong et al. (2011)
		Hazelnut	Moscetti et al. (2015)
Fluorescence	Fecal contamination	Apple	Kim et al. (2002, 2005, 2007, 2008); Lefcourt et al. (2003, 2006a); Yang et al. (2011)
		Cantaloupe	Vargas et al. (2005)
		Lettuce	Cho et al. (2018); Mo et al. (2017a)
		Spinach	Everard et al. (2014, 2016); Lefcourt and Siemens (2017); Lefcourt et al. (2019)
	Insect infestation	Lettuce	Mo et al. (2017b)
Transmittance	Insect infestation	Cherry	Xing et al. (2008)
Reflectance and fluorescence	Fecal contamination (or and surface defects)	Apple	Kim et al. (2001b, 2007, 2008); Lefcout et al. (2006b)

Reflectance and transmittance	Insect infestation	Cucumber	Lu and Ariana (2013)

Recent efforts have been devoted to detecting fecal contamination on leafy greens using hyperspectral fluorescence imaging (Cho et al., 2018; Everard et al., 2016; Everard et al., 2014; Kang et al., 2011). Compared to fruits like apple, leafy vegetables generally have more strong fluorescence emissions due to high chlorophyll concentrations, and the emissions are in proximity to those due to fecal matters in the red and far-red regions, which may require higher spectral-resolution imaging for effective detection of fecal contamination. Fecal matters exhibit slight blue shifts for the emission peak in the red region, compared to the leafy greens (Everard et al., 2014; Kang et al., 2011). In detecting cow feces on spinach, Everard et al. (2014) compared two different excitation light sources, i.e., UV-A and violet light at 405 nm. They reported that the latter performed better in detecting a range of varied dilutions of fecal contamination and that they both were superior to reflectance imaging. The authors also noted that the yellow hue or discolorations of leaves could cause false positives. It was hence suggested to image leaves before the onset of leaf deterioration (Everard et al., 2016). Cho et al. (2018) reported on the detection of four species of varied dilutions of animal feces on romaine lettuce (Cho et al., 2018), as illustrated in Figure 10. It was shown that species-specific detection after illumination with violet LED excitation light required different filters corresponding to the fluorescence emission wavelengths. The most effective two-band ratio for all species of feces was found to be 664±4 nm/694±2 nm.

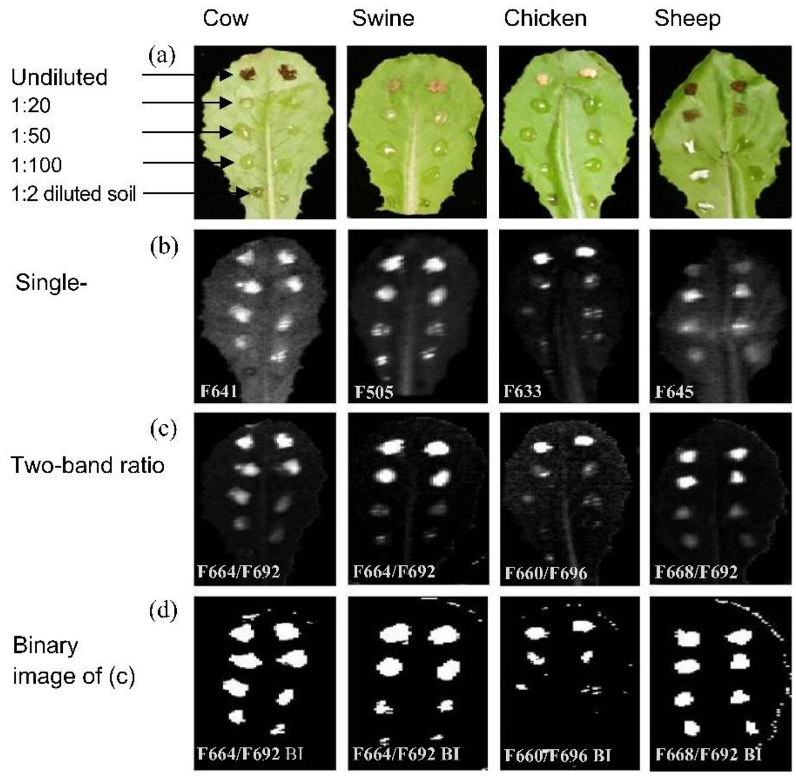

Figure 10. Detection of fecal spots from four animals (i.e., cattle, pig, chicken, and sheep) on green romaine lettuce leaves. (a) Color photos showing application locations of undiluted feces, 1:20, 1:50, and 1:100 fecal dilutions, and 1:20 dilution of soil; (b) Single waveband images for species-specific fecal detection; (c) Two-band ratio images for species-specific fecal detection; (d) Binary detection images from thresholding of the images in (c). Reproduced with permission from Cho et al. (2018).

Safety inspection for pathogenic microorganisms (or diseases) and insects is another important area of application for hyperspectral imaging. Fresh produce attacked by microorganisms will rot or decay, which may further contaminate the sound produce, resulting in substantial economic loss. Hyperspectral imaging has been used for the detection of microorganism-induced rottenness or pathogenic contaminations, discriminating infected from normal areas of food products or sorting the infected or rotten items (Gómez-Sanchis et al., 2008a; Gómez-Sanchis et al., 2014; Li et al., 2016; Siripatrawan et al., 2011; Zhang et al., 2015b). Gómez-Sanchis et al. (2008a) first reported on the detection of early rottenness in citrus fruits. Fruit decay caused by *Penicillium sp.* infection traditionally requires manual sorting under UV illumination that is harmful to operators. To avoid the use of UV lighting, they developed an LCTF-based hyperspectral imaging system with a classification accuracy of 91% by regression tree based classification. Siripatrawan et al. (2011) reported on the detection of *Escherichia coli* infection in fresh spinach and obtained prediction maps for the pathogen concentration, which allowed rapid and convenient data interpretations.

Detection of pest infestation in food products often requires performing quarantine treatments such as vapor heating or irradiation, which negatively affects food quality and consumer acceptance. Saranwong et al. (2011) reported on using hyperspectral imaging to detect fruit flies in mangoes, at the surface of which 16 small pores in a 4×4 grid pattern were created to facilitate infestation. Pixel-based Bayesian classification for three selected wavelengths yielded the best detection result 48 h after infestation. Further efforts were made to automatically identify infested regions and extend the classifications to the fruits without surface pores. i.e., no a priori knowledge of infestation locations (Haff et al., 2013). Lu and Ariana (2013) reported on detecting fruit fly infestation in pickling cucumbers using hyperspectral reflectance and transmittance imaging. Three imaging modes, i.e., reflectance (450-740 nm), transmittance (740-1000 nm) and their combination were compared for differentiating infested from normal cucumbers by PLS-DA. It was found that the transmittance imaging mode achieved the best overall accuracies of 88%-93% and that the combination mode did not produce better accuracy than transmittance. Moscetti et al. (2015) also considered insect infestation when defining the quality classes of hazelnuts to be predicted from hyperspectral images acquired in reflectance mode in the SWIR (1000-2500 nm) range. It should be noted that these infestations might be detect the changes in the optical properties of the fruit flesh rather than detecting the pest itself.

Recently, Mo et al. (2017b) developed a line-scanning hyperspectral imaging system for online detection of slugs and worms on fresh-cut lettuce. This system allowed to detect the two kinds of pests on both adaxial (upper) and abaxial (lower) surfaces of lettuce. Using image differences and ratios at selected effective wavelengths resulted in high detection rates of 98% and 99% for slugs and worms, respectively. However, the actual real-time detection speed was not mentioned in the study. More applications of hyperspectral imaging for food safety detection are listed in Table 3.

5. Challenges and Future Research Needs

Over the past 20 years, much progress has been made in the hardware and software for hyperspectral imaging, and the technology has demonstrated great capabilities in postharvest quality and safety assessment. However, critical challenges still exist and have to be addressed in future work. These challenges primarily stem from the need to develop an efficient, reliable, fast and cost-effective modality for both research purposes and practical or industrial applications.

5.1. Data Interpretation and Modeling

Large volumes of spectral-spatial data that may contain irrelevant and noisy signals, pose a great challenge in data handling and the extraction of meaningful information. Compared to spectroscopic and image data, hyperspectral image data require far more dedicated efforts on data analysis, as described in Section 3, for developing effective and reliable models. These models are typically built based on limited data acquired under well-controlled laboratory conditions, and they may not be applicable to new samples acquired in real-world situations. Hence, extensive calibration and validation based on a diversity of samples and under industry relevant conditions is needed to ensure the models are robust for practical use. An effective and reliable model requires a deep understanding of light-tissue interactions and the relations of spectral-spatial features with quality attributes to be inspected. Few reports provided in-depth analysis and discussion of the acquired data in the development of calibration models. This may result in poor generalization of the models to different application conditions. Moreover, while calibration transfer is well described for point spectroscopy systems, little research has been reported on the transferability of calibration models developed on a specific hyperspectral imaging system to other hyperspectral imaging systems which may have different imaging and/or lighting configurations. Therefore, future research is needed on the light-tissue interaction involved in hyperspectral imaging, and on the development of more effective data-mining and calibration transfer methods to fully exploit the abundant spectral-spatial information provided by the technology. In this context, it would be interesting to investigate the possibility to build self-learning correction models to overcome sample differences (varieties, harvest years, etc.) and instrumentation differences (i.e., different optical systems, light sources, imaging modes, etc.).

Hyperspectral imaging provides a unique capability and great opportunities for mapping the quality attributes or chemical composition of horticultural products in the 2-D or 3-D spatial domain. However, constructing an accurate quality or chemical composition map is not a simple task, because the models for quality prediction are typically developed using a single spectrum aggregated (e.g., by averaging) from all pixel spectra within an ROI, which may not have adequately accounted for the physical and/or physiological factors that influence the model performance. Hence, these models should be rigorously tested and validated before being used for characterizing the spatial heterogeneity within a sample. Although one may alleviate the issue by building different models, each of which is used to predict a small local area of the sample (Martinsen and Schaare, 1998; Polder et al., 2004), this approach is time consuming and also limited by actual sampling density in measuring ground-truth values. It should be noted that most published studies did not perform pixel-level accuracy validation for the mapping results, mainly due to the difficulty of obtaining pixel-level ground-truth values. Hence, future research is needed on new modeling methods and validation strategies for more accurate mapping of quality attributes or chemical composition.

5.2. Real-time, Online Applications

Besides equipment cost, speed is presumably the most critical factor in commercial adoption of hyperspectral imaging technology for real-time inspection of horticultural commodities. The inspection speed by hyperspectral imaging is constrained by the time needed to acquire, transfer and analyze large volumes of image data (at tens to hundreds of wavelengths), each of which could be the limiting factor for achieving a practical inspection rate (e.g., 5-10 or more food items per second). While the recent advancements in hardware and software have greatly improved the implementation speed of hyperspectral imaging, compared to 20 years ago, there are still relatively few real-time implementations of hyperspectral imaging for postharvest quality inspection. One technically feasible solution is to configure a line-scanning hyperspectral imaging system in a multispectral mode (or hyperspectral-multispectral mode). This approach is advantageous for online applications, in terms of speed and flexibility, compared to the conventional multispectral imaging approach, and hence it should be further considered for online inspection of horticultural products. Real-time inspection rates of about 3 items per second have been reported by implementing line-scan hyper-multispectral imaging for poultry carcass inspection (Park and Yoon, 2015; Yoon et al., 2011), but the speed still falls short of the requirement for inspecting horticultural commodities. Moreover, defect detection for round-shaped horticultural commodities such as apples requires inspecting the whole product surface. This requires fast rotating of products during image acquisition, as is already done in conventional machine vision systems. The implementation of fruit rotation for hyperspectral line-scanning is challenging, but technically possible. High-speed, high performance imaging cameras currently are available to meet the need of scanning rotating horticultural products, although costs are still high.

Integrated imaging modes (i.e., reflectance and transmittance, and reflectance and fluorescence) expand the capabilities of hyperspectral imaging for multi-parameter inspection (Kim et al., 2008). Coupled with the hyperspectral-multispectral mode, these integrated imaging modes could provide new opportunities for online inspection of postharvest quality and safety of horticultural products. As discussed in Section 2.4.2, snapshot hyperspectral imaging holds great promise for real-time postharvest quality and safety inspection, owing to its ability of acquiring hyperspectral image cubes simultaneously. The technology is evolving rapidly, and some devices are already commercially available and have started to find applications in the fields of remote sensing and biomedical imaging. At present, most snapshot cameras on the market are based on CMOS sensors. It remains to be evaluated whether these cameras are able to deliver sufficiently high-quality images at the wavelengths of interest for real-time applications.

In addition, miniaturized, handheld hyperspectral imaging devices, either snapshot or internal line-scanning based, have emerged recently (Behmann et al., 2018; Wu et al., 2014). These devices provide convenience and new opportunities for fast, on-site inspection, but their performance remains to be evaluated.

In recent years, fast computing technologies based on parallel computing have evolved rapidly, which provides a means for accelerating hyperspectral-related computations (Burger and Gowen, 2011; Plaza and Plaza, 2011). Parallel computing, which allows simultaneous use of computer resources [e.g., multiple central processing units (CPUs) in a computer], can execute multiple tasks simultaneously and is thus well suited for multi-tasking food quality and safety inspection by hyperspectral imaging. In particular, parallel computing, using field programmable gate arrays (FPGAs) and graphical processing units (GPUs), has demonstrated excellent performance in hyperspectral remote sensing applications (Bernabe et al., 2013; Ghamisi et al., 2017) and is currently used in commercial postharvest sorting systems based on hyperspectral imaging. Owing to the advancements in computing technologies, especially the utilization of GPUs along with deep learning frameworks (e.g., TensorFlow, PyTorch, Caffe and Theano), deep neural networks (DNNs) that are inherently computationally intensive, are becoming increasingly popular in solving computer vision tasks with superior accuracies. Efficient deployment of DNNs based on GPU accelerations (Sze et al., 2017) is likely to greatly enhance the capacity of hyperspectral imaging for detecting different types of defects in horticultural products, which, however, require a sufficiently large image dataset to train the networks. Hence, future research efforts should also be directed at efficient utilization of DNNs for rapid and effective defect detection in horticultural products.

6. Conclusions

Since its introduction for postharvest quality and safety assessment in the late 1990s, hyperspectral imaging technology has been extensively researched for external quality and defect detection, internal quality and maturity assessment, and food safety inspection. Great progress in the hardware design and implementation and image processing algorithms and methodologies has been made over the past 20 years, and several online hyperspectral imaging prototypes have been developed for horticultural products. However, commercial application of the technology has been slow in progress, due to the constraints in image acquisition and processing speed and equipment cost. With the further advancement in imaging implementation modes and the emergence of new imaging modalities (i.e., snapshot and miniaturized, portable devices), along with new, faster and more powerful image processing and computing techniques including artificial intelligence, hyperspectral imaging technology will find more wide applications in the near future for enhanced quality and safety evaluation of horticultural products, especially at the industry scale.

References

Ariana, D., Guyer, D., Shrestha, B., 2006. Integrating multispectral reflectance and fluorescence imaging for defect detection on apples. Computers and Electronics in Agriculture 50, 148-161.

Ariana, D.P., Lu, R., 2008a. Detection of internal defect in pickling cucumbers using hyperspectral transmittance imaging. Transactions of the ASABE 51, 705-713.

Ariana, D.P., Lu, R., 2008b. Quality evaluation of pickling cucumbers using hyperspectral reflectance and transmittance imaging: Part I. Development of a prototype. Sensing and Instrumentation for Food Quality and Safety 2, 144-151.

Ariana, D.P., Lu, R., 2008c. Quality evaluation of pickling cucumbers using hyperspectral reflectance and transmittance imaging: Part II. Performance of a prototype. Sensing and Instrumentation for Food Quality and Safety 2, 152-160.

Ariana, D.P., Lu, R., 2010. Evaluation of internal defect and surface color of whole pickles using hyperspectral imaging. Journal of Food Engineering 96, 583-590.

Arici, T., Dikbas, S., Altunbasak, Y., 2009. A histogram modification framework and its application for image contrast enhancement. IEEE Transactions on Image Processing 18, 1921-1935.

Baranowski, P., Mazurek, W., Pastuszka-Woźniak, J., 2013. Supervised classification of bruised apples with repect to the time after bruising on the basis of hyperspectral imaging data. Postharvest Biology and Technology 86, 249-258.

Barens, R.J., Dhanoa, M.S., Lister, S.J., 1989. Standard normal variate transformation and de-trending of near-infrared diffuse reflectance spectra. Applied Spectroscopy 43, 772-777.

Behmann, J., Acebron, K., Emin, D., Bennertz, S., Matsubara, S., Thomas, S., Bohnenkamp, D., Kuska, M.T., Jussila, J., Salo, H., Mahlein, A.K., Rascher, U., 2018. Specim IQ: evaluation of a new, miniaturized handheld hyperspectral camera and its application for plant phenotyping and disease detection. Sensors 18, 441.

Bernabe, S., lopez, S., Plaza, A., Sarmiento, R., 2013. GPU implementation of an automatic target detection and classification algorithm for hyperspectral image analysis. IEEE Geoscience and Remote Sensing Letters 10, 221-225.

Birlouez-Aragon, I., Buschmann, C., Hashimoto, A., Kameoka, T., Kumke, M.U., Lakhal, L., Langsdorf, G., Lichtenthaler, H.K., Lohmannsroben, H.G., Rizkallaf, J., Saito, Y., 2008. Fluoresence, In: Zude, M. (Ed.), Optical Monitoring of Fresh and Processed Agricultural Crops. CRC Press, Boca Raton, FL, USA., pp. 251-375.

Breiman, L., 2001. Random forests. Machine Learning 45, 5-32.

Brosnan, T., Sun, D.W., 2004. Improving quality inspection of food products by computer vision: a review. Journal of Food Engineering 61, 3-16.

Burger, J., Gowen, A., 2011. Data handling in hyperspectral image analysis. Chemometrics and Intelligent Laboratory Systems 108, 13-22.

Buschmann, C., Langsdorf, G., Lichtenthaler, H.K., 2000. Imaging of the blue, green, and red fluorescence emission of plants: an overview. Photosynthetica 38, 483-491.

Buschmann, C., Lichtenthaler, H.K., 1998. Principles and characteristics of multi-colour fluorescence imaging of plants. Journal of Plant Physiology 152, 297-314.

Celik, T., 2012. Two-dimensionalhistogramequalizationandcontrastenhancement. Pattern Recognition 45, 3810-3824.

Cen, H., Lu, R., Ariana, D.P., Mendoza, F., 2014. Hyperspectral imaging based classification and wavebands selection for internal defect detection of pickling cucumbers. Food and Bioprocess Technology 7, 1689-1700.

Cen, H., Lu, R., Mendoza, F.A., Ariana, D.P., 2012. Assessing multiple quality attributes of peaches using optical absorption and scattering properties. Transactions of the ASABE 55, 647-657.

Cen, H., Lu, R., Zhu, Q., Mendoza, F., 2016. Nondestructive detection of chilling injury in cucumber fruit using hyperspectral imaging with feature selection and supervised classification. Postharvest Biology and Technology 111, 352-361.

Centner, V., Massart, D.L., de Noord, O.E., de Jong, S., 1996. Elimination of uninformative variables for multivariate calibration. Analytical Chemistry 68, 3851-3858.

Chandrashekar, G., Sahin, F., 2014. A survey on feature selection methods. Computers and Electrical Engineering 40, 16-28.

Chao, K., Chen, Y.R., Kim, M.S., Chan, D., Yang, C.C., 2014. Method and system for wholesomeness inspection of freshly slaughtered chickens on a processing line, USA.

Chao, K., Yang, C.C., Chen, Y.R., Kim, M.S., Chan, D.E., 2007. Hyperspectral/multispectral line-scan imaging sytem for automated poultry carcass inpsection applications for food safety. Poultry Science 86, 2450-2460.

Chao, K., Yang, C.C., Kim, M.S., 2010. Spectral line-scan imaging system for high-speed non-destructive wholesomeness insepction of broilers. Trends in Food Science & Technology 21, 129-137.

Cheng, X., Chen, Y.R., Tao, Y., Wang, C.Y., Kim, M.S., Lefcourt, A.M., 2004. A novel integrated PCA and FLD method on hyperspectral image feature extraction for cucumber chilling damage inspection. Transactions of the ASAE 47, 1313-1320.

Cho, H., Kim, M.S., Kim, S., Lee, H., Oh, M., Chung, S.H., 2018. Hyperspectral determination of fluorescence wavebands for multispectral imaging detection of multiple animal fecal species contaminations on romaine lettuce. Food and Bioprocess Technology 11, 774-784.

Clark, C.J., McGlone, V.A., Jordan, R.B., 2003. Detection of brownheart in 'Braeburn', apple by transmission NIR spectroscopy. Postharvest Biology and Technology 28, 87-96.

Cowe, I., A., McNIcol, J. W., 1985. The use of principal components in the analysis of near-infrared spectra. Applied Spectroscopy 39, 257-266.

Cubero, S., Aleixos, N., Molto, E., Gomez-Sanchis, J., Blasco, J., 2011. Advances in machine vision applications for automatic insepction and quality evaluation of fruits and vegetables. Food and Bioprocess Technology 4, 487-507.

Díaz-Uriarte, R., de Andrés, S.A., 2006. Gene selection and classification of microarray data using random forest. BMC Bioinformatics 7, 3.

ElMasry, G., Wang, N., ElSayed, A., Ngadi, M., 2007. Hyperspectral imaging for nondestructive determination of some quality attributes for strawberry. Journal of Food Engineering 81, 98-107.

ElMasry, G., Wang, N., Vigneault, C., 2009. Detecting chilling injury in Red Delicious apple using hyperspectral imaging and neural networks. Postharvest Biology and Technology 52, 1-8.

ElMasry, G., Wang, N., Vigneault, C., Qiao, J., ElSayed, A., 2008. Early detection of apple bruises on diffeent background colors using hyperspectral imaging. LWT - Food Science and Technology 41, 337-345.

Everard, C.D., KIm, M.S., Cho, H., O'Donnell, C.P., 2016. Hyperspectral fluorescence imaging using violet LEDs as excitation sources for fecal matter contaminate identification on spinach leaves. Food Measure 10, 56-63.

Everard, C.D., Kim, M.S., Lee, H., 2014. A comparison of hyperspectral reflectance and fluorescence imaging techniques for detection of contaminants on spinach leaves. Journal of Food Engineering 143, 139-145.

Fan, X., Huang, W., Guo, Z., Zhang, B., Zhao, C., 2015. Prediction of soluble solids content and firmness of pears using hyperspectral reflectance imaging. Food Analytical Methods 8, 1936-1946.

Fernandes, A.M., Oliveira, P., Moura, J.P., Oliveira, A.A., Falco, V., Correia, M.J., Melo-Pinto, P., 2011. Determination of anthocyanin concentration in whole grape skins using hyperspectral imaging and adaptive boosting neural networks. Journal of Food Engineering 105, 216-226.

Geelen, B., Blanch, C., Gonzalez, P., Tack, N., Lambrechts, A., 2015. A tiny, VIS-NIR snapshot multispectral camera, Advanced Fabrication Technologies for Micro/Nano Optics and Photonics VIII. Proc. of SPIE, San Francisco, CA, USA.

Geelen, B., Tack, N., Lambrechts, A., 2013. A snapshot multispectral imager with integrated, tiled filters and optical duplication, In: von Freymann, G., Schoenfeld, W.V., Rumpf, R.C. (Eds.), Proceedings Volume 8613, Advanced Fabrication Technologies for Micro/Nano Optics and Photonics VI. Proc. of SPIE, San Francisco, CA, USA.

Geelen, B., Tack, N., Lambrechts, A., 2014. A compact snapshot multispectral imager with a monolithically integrated, per-pixel filter mosic, In: von Freymann, G., Schoenfeld, W.V., Rumpf, R.C. (Eds.), Advanced Fabrication Technologies for Micro/Nano Optics and Photonics VII. Proc. of SPIE, San Francisco, CA, USA. .

Ghamisi, P., Yokoya, N., Li, J., Liao, W., Liu, S., Plaza, J., Rasti, B., Plaza, A., 2017. Advances in hyperspectral imaging and signal processing: a comprehensive overview of the state of the art. IEEE Geoscience and Remote Sensing Magazine 5, 37-78.

Goetz, A.F.H., Vane, G., Solomon, T.E., Rock, B.N., 1985. Imaging spectrometry for earth remote sensing. Science 228, 1147-1153.

Golding, J., Wills, R., 2016. Postharvest: an introduction to the physiology and handling of fruit and vegetables. UNSW Press, Sydney, Australia.

Gómez-Sanchis, J., Blasco, J., Soria-Olivas, E., Lorente, D., Escandell-Montero, P., Martínez-Martínez, J.M., Martínez-Sober, M., Aleixos, N., 2013. Hyperspectral LCTF-based system for classification of decay in mandarins caused by Penicillium digitatum and Penicillium italicum using the most relevant bands and non-linear classifiers. Postharvest Biology and Technology 82, 76-86.

Gómez-Sanchis, J., Gomez-Chova, L., Aleixos, N., Camps-Valls, G., Montesinos-Herrero, C., Molto, E., Blasco, J., 2008a. Hyperspectral system for early detection of rottenness caused by *Penicillium digitatum* in mandarins. Journal of Food Engineering 89, 80-86.

Gómez-Sanchis, J., Lorente, D., Soria-Olivas, E., Aleixos, N., Cubero, S., Blasco, J., 2014. Development of a hyperspectral computer vision system based on two liquid crystal tuneable filters for fruit inspection. application to detect citrus fruits decay. Food and Bioprocess Technology 7, 1047-1056.

Gómez-Sanchis, J., Molto, E., Camps-Valls, G., Gomez-Chova, L., Aleixos, N., Blasco, J., 2008b. Automatic correction of the effects of the light source on spherical objects. An application to the analysis of hyperspectral images of citrus fruits. Journal of Food Engineering 85, 191-200.

Gonzalez, R.C., Woods, R.E., 2008. Digital Image Processing. Pearson Education, London, UK.

Gowen, A.A., O'Donnell, C.P., Cullen, P.J., Downey, G., Frias, J.M., 2007. Hyperspectral imaging: an emerging process analytical tool for food quality and safety control. Trends in Food Science & Technology 18, 590-598.

Gowen, A.A., O'Donnell, C.P., Taghizadeh, M., Cullen, P.J., Frias, J.M., Downey, G. 2008. Hyperspectral imaging combined with principal component analysis for bruise damage detection on white mushrooms (*Agaricus bisporus)*. Journal of Chemometrics 22, 259-267.

Green, A.A., Berman, M., Switzer, P., Craig, M.D., 1988. A transformation for ordering multispectral data in term of image quality with implications for noise removal. IEEE Transactions on Geoscience and Remote Sensing 26, 65-74.

Guo, W., Zhao, F., Dong, J., 2015. Nondestructive measurement of soluble solids content of kiwifruits using near-infrared hyperspectral imaging. Food Analytical Methods 9, 38-47.

Guyon, I., Elisseeff, A., 2003. An introduction to variable and feature selection. Journal of Machine Learning Research 3, 1157-1182.

Guyon, I., Weston, J., Barnhill, S., Vapnik, V., 2002. Gene selection for cancer classification using support vector machine. Machine Learning 46, 389-422.

Haff, R.P., Saranwong, S., Thanapase, W., Janhiran, A., Kasemsumran, S., Kawano, S., 2013. Automatic image analysis and spot classification for detection of fruitfly infestation in hyperspectral images of mangoes. Postharvest Biology and Technology 86, 23-28.

Hagen, N., Kudenov, M.W., 2013. Review of snapshot spectral imaging technologies. Optical Engineering 52, 090901.

Han, D., Tu, R., Lu, C., Liu, X., Wen, Z., 2006. Nondestructive detection of brown core in the Chinese pear 'Yali' by transmission visible–NIR spectroscopy. Food Control 17, 604-608.

Haralick, R.M., 1979. Statistical and structural approaches to texture. Proceedings of the IEEE 67, 786-804.

Hastie, T., Tibshirani, R., Friedman, J., 2009. The Elements of Statistical Learning: Data Mining, Inference, and Prediction. Springer-Verlag, New York.

Huang, M., Lu, R., 2010. Apple mealiness detection using hyperspectral scattering technique. Postharvest Biology and Technology 58, 168-175.

Huang, M., Wan, X., Zhan, M., Zhu, Q., 2013. Detection of insect-damaged vegetable soybeans using hyperspectral. Journal of Food Engineering 116, 45-49.

Isaksson, T., Næs, T., 1988. The effect of multiplicative scatter correction (MSC) and linearity improvement in NIR spectroscopy. Applied Spectroscopy 42, 1273-1284.

Kamarainen, J.K., Kyrki, V., Kalviainen, H., 2006. Invariance properties of gabor gilter-based features—overview and applications. IEEE Transactions on Image Processing 15, 1088-1099.

Kang, S., Lee, K., Son, J., Kim, M.S., 2011. Detection of fecal contamination on leafy greens by hyperspectral imaging. Procedia Food Science 1, 953-959.

Kavdir, I., Guyer, D.E., 2008. Evaluation of different pattern recognition techniques for apple sorting. . Biosystems Engineering 99, 211-219.

Keresztes, J.C., Diels, E., Goodarzi, M., Nguyen, N., Goos, P., Nicolai, B., Saeys, W., 2017. Glare based apple sorting and iterative algorithm for bruise region detection using shortwave infrared hyperspectral imaging. Postharvest Biology and Technology 130, 103-115.

Keresztes, J.C., Goodarzi, M., Saeys, W., 2016a. Real-time pixel based early apple bruise detection using short wave infrared hyperspectral imaging in combination with calibration and glare correction technique. Postharvest Biology and Technology 66, 215-226.

Keresztes, J.C., Koshel, R.J., D'huys, K., De Ketelaere, B., Audenaert, J., Goos, P., Saeys, W., 2016b. Augmented design and analysis of computer experiments: a novel tolerance embedded global optimization approach applied to SWIR hyperspectral illumination design. Optics Express 24, 29380-29405. 24, 29380-29405.

Kester, R.T., Bedard, N., Gao, L., Tkaczyk, T.S., 2011. Real-time snapshot hyperspectral imaging endoscope. Journal of Biomedical Optics 16, 056005.

Khodabakhshian, R., Emadi, B., 2018. Application of VIS/SNIR hyperspectral imaging in ripeness classification of pear. International Journal of Food Properties 20, 3149-3163.

Kim, M.S., 2015. Online screening of fruits and vegetables using hyperspectral line-scan imaging technique, In: Bhunia, A.K., Kim, M.S., Taitt, C.R. (Eds.), High throughput screening for food safety assessment. Woodhead Publishing, Cambridge, UK, pp. 467-490.

Kim, M.S., Chao, K., Chen, Y.R., Chan, D., Mehl, P.M., 2001a. Hyperspectral imaging system for food safety: detection of fecal contamination on apples, In: Chen, Y.R., Tu, S.I. (Eds.), Photonic Detection and Intervention Technologies for Safe Food. SPIE, Boston, MA, USA.

Kim, M.S., Chen, Y.R., Cho, B.K., Chao, K., Yang, C.C., Lefcourt, A.M., Chan, D., 2007. Hyperspectral reflectance and fluorescence line-scan imaging for online defect and fecal contamination inspection of apples. Sensing and Instrumentation for Food Quality and Safety 1, 151-159.

Kim, M.S., Chen, Y.R., Mehl, P.M., 2001b. Hyperspectral reflectance andd fluoresence imaging system for food quality and safety. Transactions of the ASAE 44, 721-729.

Kim, M.S., Lee, K., Chao, K., Lefcourt, A.M., Jun, W., Chan, D.E., 2008. Multispectral line-scan imaging system for simultaneous fluoresence and reflectance measurement of apples: multitask apple inspection system Sensing and Instrumentation for Food Quality and Safety 2, 123-129.

Kim, M.S., Lefcourt, A.M., Chen, Y.R., Kang, S., 2004. Uses of hyperspectral and multispectral laser Induced fluorescence imaging techniques for food safety inspection. Eey Engineering Materials 270-273, 1055-1063.

Kim, M.S., Lefcourt, A.M., Chen, Y.R., Kim, I., Chan, D.E., Chao, K., 2002. Multispectral detection of fecal contamination on apples based on hyperspectral imagery: Part II. Application of hyperspectral fluorescence imaging. Transactions of the ASAE 45, 2039-2047.

Kim, M.S., Lefcourt, A.M., Chen, Y.R., Tao, Y., 2005. Automated detection of fecal contamination of apples based on multispectral fluorescence image fusion. Journal of Food Engineering 71, 85-91.

Kleynen, O., Leemans, V., Destain, M.F., 2005. Development of a multi-spectral vision system for the detection of defects on apples. Journal of Food Engineering 69, 41-49.

Lange, H., 2005. Automatic glare removal in reflectance imagery of the uterine cervix. Proceedings of SPIE 5747, Medical Imaging: Image Processing, (29 April 2005), https://doi.org/10.1117/12.596012.

Leardi, R., González, A.L., 1998. Genetic algorithms applied to feature selection in PLS regression: how and when to use them. Chemometrics and Intelligent Laboratory Systems 41, 195-207.

LeCun, Y., Bengio, Y., Hinton, G., 2015. Deep leaning. Nature 521, 436-444.

Lee, J.B., Woodyatt, A.S., Berman, M., 1990. Enhancement of high spectral resolution remote-sensing data by a noise-adjusted principal components transform. IEEE Transactions on Geoscience and Remote Sensing 28, 295-305.

Lee, K., Kang, S., Delwiche, S.R., Kim, M.S., Noh, S., 2008. Correlation analysis of hyperspectral imagery for multispectral wavelength selecdtion for detection of defects on apples. Sensing and Instrumentation for Food Quality and Safety 2, 90-96.

Leemans, V., Destain, M.F., 2004. A real-time grading method of apples based on features extracted from defects. Journal of Food Engineering 61, 83-89.

Lefcourt, A.M., Kim, M.S., 2006a. Technique for normalizing intensity histograms of images when the approximate size of the target is known: detection of feces on apples using fluorescence imaging. Computers and Electronics in Agriculture 50, 135-147.

Lefcourt, A.M., Kim, M.S., Chen, Y.R., 2003. Automated detection of fecal contamination of apples by multispectral laser-induced fluorescence imaging. Applied Optics 42, 3935-3943.

Lefcourt, A.M., Kim, M.S., Chen, Y.R., Kang, S., 2006b. Systematic approach for using hyperspectral imaging data to develop multispectral imagining systems: detection of feces on apples. Computers and Electronics in Agriculture 54, 22-35.

Lefcourt, A.M., Siemens, M.C., 2017. Interactions of insolation and shading on ability to use fluorescence imaging to detect fecal contaminated spinach. Applied Sciences 10, 1041.

Lefcourt, A.M., Siemens, M.C., Rivadeneira, P., 2019. Optical parameters for using visible-wavelength reflectance or fluorescence imaging to detect bird excrements in produce fields. Applie Sciences 9, 715.

Leiva-Valenzuela, G.A., Lu, R., Aguilera, J.M., 2013. Prediction of firmness and soluble solids content of blueberries using hyperspectral reflectance imaging. Journal of Food Engineering 115, 91-98.

Leiva-Valenzuela, G.A., Lu, R., Aguilera, J.M., 2014. Assessment of internal quality of blueberries using hyperspectral transmittance and reflectance images with whole sepctra or selected wavebands. Innovative Food Science and Emerging Technologies 24, 2-13.

Li, B., Cobo-Medina, M., Lecourt, J., Harrison, N., Harrison, R.J., Cross, J.V., 2018. Application of hyperspectral imaging for nondestructive measurement of plum quality attributes. Postharvest Biology and Technology 141, 8-15.

Li, H., Liang, Y., Xu, Q., Cao, D., 2009. Key wavelengths screening using competitive adaptive reweighted sampling method for multivariate calibration. Analytica Chimica Acta 648, 77-84.

Li, J., Huang, W., Tian, X.W., C., Fan, S., Zhao, C., 2016. Fast detection and visualization of early decay in citrus using Vis-NIR hyperspectral imaging. Computers and Electronics in Agriculture 127, 582-592.

Li, J., Luo, W., Wang, Z., Fan, S., 2019. Early detection of decay on apples using hyperspectral reflectance imaging combining both principal component analysis and improved watershed segmentation method. Postharvest Biology and Technology 149, 235-246.

Li, J., Rao, X., Ying, Y., 2011. Detection of common defects on oranges using hyperspectral reflectance imaging. Computers and Electronics in Agriculture 78, 38-48.

Lichtenthaler, H.K., Miehe, J.A., 1997. Fluorescence imaging as a diagnostic tool for plant stress. Trends in Plant Science 2, 316-320.

Liu, Q., Zhou, D., Tu, S., Xiao, H., Zhang, B., Sun, Y, Pan, L., Tu K., 2020. Quantitative visualization of fungal contamination in peach fruit using hyperspectral imaging. Food Analyitical Methods https://doi.org/10.1007/s12161-020-01747-x.

Liu, Y., Chen, Y.R., Wang, C.Y., Chan, D.E., Kim, M.S., 2005. Development of a simple algorithm for the detection of chilling injury in cucumbers from visible/near-infrared hyperspectral imaging. Applied Spectroscopy 59, 78-85.

Liu, Y., Chen, Y.R., Wang, C.Y., Chan, D.E., Kim, M.S., 2007. Development of hyperspectral imaging technique for the detection of chilling injury in cucumbers: spectral and image analysis. Applied Engineering in Agriculture 22, 101-111.

Lleó, L., Roger, J.M., Herrero-Langreo, A., Diezma-Iglesias, B., Barreiro, P., 2011. Comparison of multispectral indexes extracted from hyperspectral images for the assessment of fruit ripening. Journal of Food Engineering 104, 612-620.

Lopez-Maestresalas, A., Keresztes, J.C., Goodarzi, M., Arazuri, S., Jaren, C., Saeys, W., 2016. Non-destructive detection of blackspots in potatoes by Vis-NIR and SWIR hyperspectral imaging. Food Control 70, 229-241.

Lu, R., 2003. Detection of bruises on apples using near-infrared hyperspectral imaging. Transactions of the ASAE 46, 523-530.

Lu, R., 2004. Multispectral imaging for predicting firmness and soluble solids content of apple fruit. Postharvest Biology and Technology 31, 147-157.

Lu, R., 2007. Nondestructive measurement of firmness and soluble solids content for apple fruit using hyperspectral scattering images. Sensing and Instrumentation for Food Quality and Safety 1, 19-27.

Lu, R., Ariana, D.P., 2013. Detection of fruit fly infestation in pickling cucumbers using a hyperspectral reflectance/transmittance imaging system Postharvest Biology and Technology 81, 44-50.

Lu, R., Chen, Y.R., 1998. Hyperspectral imaging for safety inspection of food and agricultural products, SPIE Conference on Pathogen Detection and Remediation for Safe Eating. SPIE, Boston, MA, USA, pp. 121-133.

Lu, R., Chen, Y.R., Park, B., Choi, K.H., 1999. Hyperspectral imaging for detecting bruises in apples, ASAE Annual International Meeting Toronto, Ontario, Canada.

Lu, R., Peng, Y., 2006. Hyperspectral scattering for assessing peach fruit firmness. Biosystems Engineering 93, 161-171.

Lu, R., van Beers, R., Saeys, W., Li, C., Cen, H., 2020. Measurement of optical properties of fruits and vegetables: A review. Postharvest Biology and Technology 159, 111003.

Lu, Y., Huang, Y., Lu, R., 2017. Innovative hyperspectral imaging-based techniques for quality evaluation of fruits and vegetables: a review. Applied Sciences 7, 189.

Lu, Y., Lu, R., 2017a. Development of a multispectral structured illumination reflectance imaging (SIRI) system and its application to bruise detection of apples. Transactions of the ASABE 60, 1379-1389.

Lu, Y., Lu, R., 2017b. Histogram-based automatic thresholding for bruise detection of apples by structured-illumination reflectance imaging. Biosystems Engineering 160, 30-41.

Lu, Y., Lu, R., 2017c. Non-destructive defect detection of apples by spectroscopic and imaging technologies: a review. Transactions of the ASABE 60, 1765-1790.

Lu, Y., Lu, R., 2018a. Detection of surface and subsurface defects of apples using structured-illumination reflectance imaging with machine learning algorithms. Transactions of the ASABE 61, 1831-1842.

Lu, Y., Lu, R., 2018b. Fast bi-dimensional empirical mode decomposition as an image enhancement technique for fruit defect detection. Computers and Electronics in Agriculture 152, 314-323.

Ma, T., Li, X., Inagaki, T., Yang, H., Tsuchikawa, S., 2018. Noncontact evaluation of soluble solids content in apples by near-infrared hyperspectral imaging. Journal of Food Engineering 224, 53-61.

Maldonado, S., Weber, R., Basak, J., 2011. Simultaneous feature selection and classification using kernel-penalized support vector machines. Information Sciences 181, 115-128.

Marsland, S., 2015. Machine learning: an algorithmic perspective (second edition). CRC Press, Baco Raton, FL, USA.

Martinsen, P., Schaare, P., 1998. Measuring soluble solids distribution in kiwifruit using near-infrared imaging spectroscopy. Postharvest Biology and Technology 14, 271-281.

Matousek, P., Morris, M.D., 2010. Emerging Raman applications and techniques in biomedical and pharmaceutical fields. Springer, Berlin, Germany.

Mehl, P.M., Chao, K., Kim, M., Chen, Y.R., 2002. Detection of defects on selected apple cultivars using hyperspectral and mulitispectral image analysis. Applied Engineering in Agriculture 18, 219-226.

Mehl, P.M., Chen, Y.R., Kim, M.S., Chan, D.E., 2004. Development of hyperspectral imaging technique for the detection of apple surface defects and contaminations. Journal of Food Engineering 61, 67-81.

Mendoza, F., Lu, R., Ariana, D.P., Cen, H. and Bailey, B.B., 2011. Integrated spectral and image analysis of hyperspectral scattering data for predicting apple fruit firmness and soluble solids content. Postharvest Biology and Technology 62, 149-160.

Mendoza, F., Lu, R., Cen, H., 2012. Comparison and fusion of four nondestructive sensors for predicting apple fruit firmness and soluble solids content. Postharvest Biology and Technology 73, 89-98.

Mendoza, F., Lu, R., Cen, H., 2014. Grading of apples based on firmness and soluble solids content using Vis/SWNIR spectroscopy and spectral scattering techniques. . Journal of Food Engineering 125, 59-68.

Menesatti, P., Zanella, A., D'Andrea, S. Costa, C., Paglia, G., Pallottino, F., 2008. Supervised multivariate analysis of hyper-spectral NIR images to evaluate the starch index of apples. Food and Bioprocess Technology 2, 308-314.

Mo, C., Kim, G., Kim, M.S., Lim, J., Cho, H., Barnaby, J.Y., Cho, B.K., 2017a. Fluorescence hyperspectral imaging technique for foreign substance detection on fresh-cut lettuce. Journal of the Science of Food and Agriculture 97, 3985-9993.

Mo, C., Kim, G., Kim, M.S., Lim, J., Lee, K., Lee, W., Cho, B., 2017b. On-line fresh-cut lettuce quality measurement system using hyperspectral imaging. Biosystems Engineering 156, 38-50.

Mo, C., Kim, G., Lim, J., Kim, M.S., Cho, H., Cho, B.K., 2015. Detection of lettuce discoloration using hyperspectral reflectance imaging. Sensors 15, 29511-29534.

Moscetti, R., Saeys, W., Keresztes, J.C., Goodarzi, M., Cecchini, M., Danilo, M., Massantini, R., 2015. Hazelnut quality sorting using high dynamic range short-wave infrared hyperspectral imaging. Food and Bioprocess Technology 8, 1593-1604.

Munera, S., Besada, C., Blasco, J., Cubero, S., Salvador, A., Talens, P., Aleixos, N., 2017. Astringency assessment of persimmon by hyperspectral imaging. Postharvest Biology and Technology 125, 35-41.

Munera, S. Blasco, J., Amigo, J. M., Cubero, S., Talens, P., Aleixos, N., 2019. Use of hyperspectral transmittance imaging to evaluate the internal quality of nectarines. Biosystems Engineering 182, 54-64.

Nagata, M., Tallada, J.G., Kobayashi, T., 2006. Bruise detection using NIR hyperspectral imaging for strawberry (Fragaria×ananassa Duch.). 2006 44, 133-142.

Nagata, M., Tallada, J.G., Kobayashi, T., Cui, Y., Gejima, Y., 2004. Prediction maturity quality parameters of strawberries using hyperspectral imaging, ASAE Annual International Meeting, Ottawa, Ontario, Canada.

Nicolaï, B.M., Beullens, K., Bobelyn, E., Peirs, A., Saeys, W., Theron, K.I., Lammertyn, J., 2007. Nondestructive measurement of fruit and vegetable quality by means of NIR spectroscopy: A review. . Postharvest Biology and Technology 46, 99-118.

Nicolaï, B.M., Lötze, E., Peirs, A., Scheerlinck, N., Theron, K.I., 2006. Non-destructive measurement of bitter pit in apple fruit using NIR hyperspectral imaging. Postharvest Biology and Technology 40, 1-6.

Nixon, M.S., Aguado, A.S., 2012. Feature extraction and image processing for computer visiion (3rd ed.). Elsevier, Singapore.

Noh, H.K., Lu, R., 2007. Hyperspectral laser-induced fluoresence imaging for assessing apple fruit quality. Postharvest Biology and Technology 43, 193-201.

Noh, H.K., Peng, Y., Lu, R., 2007. Integration of hyperspectral reflectance and fluorescence imaging for assessing apple maturity. Transactions of the ASABE 50, 963-971.

Noordam, J.C., van den Broek, W.H.A.M., Buydens, L.M.C., 2004. Perspective of inline control of latent defects and diseases on French Fries with multispectral imaging., In: Y.R., C., Meyer, G.E. (Eds.), Food Safety and Agricultural Monitoring. SPIE, Providence, Rhode Island, USA.

Norgaard, L., Saudland, A., Wanger, J., Nielsen, J., Munck, L., Engelsen, S., 2000. Interval partial least-squares regression (iPLS): a comparative chemometricstudywith anexamplefromnear-infrared spectroscopy. . Applied Spectroscopy 54, 413-419.

Ojala, T., Pietikainen, M., Maenpaa, T., 2002. Multiresolution gray-scale and rotation invariant texture classification with local binary patterns. IEEE Transactions on Pattern Analysis and Machine Intelligence 24, 971-987.

Pan, L., Sun, Y., Xiao, H., Gu, X., Hu, P., Wei, Y., Tu, K., 2017. Hyperspectral imaging with different illumination patterns for the hollowness classification of white radish. Postharvest Biology and Technology 126, 40-49.

Pan, L., Zhang, Q., Zhang, W., Sun, Y., Hu, P., Tu, K., 2016. Detection of cold injury in peaches by hyperspectral reflectance imaging and artificial neural network. Food Chemistry 192, 134-141.

Park, B., Yoon, S.C., 2015. Real-time hyperspectral imaging for food safety, In: Park, B., Lu, R. (Eds.), Hyperspectral imaging technology in food and agriculture. Springer, New York, USA, pp. 305-329.

Park, B., Yoon, S.C., Windham, W.R., Lawrence, K.C., Kim, M.S., Chao, K., 2011. Line-scan hyperspectral imaging for real-time in-line poultry fecal detection Sensing and Instrumentation for Food Quality and Safety 5, 25-32.

Peirs, A., Scheerlinck, N., De Baerdemaeker, J., Nicolaï, B.M., 2003. Starch index determination of apple fruit by means of a hyperspectral near infrared reflectance imaging system. Journal of Near Infrared Spectroscopy 11, 379-389.

Peng, Y., Lu, R., 2008. Analysis of spatially resolved hyperspectral scattering images for assessing apple fruit firmness and soluble solids content. Postharvest Biology and Technology 48, 52-62.

Pichette, J., Lanrence, A., Angulo, L., Lesage, F., Bouthillier, A., Nguyen, D.K., Leblond, F., 2016. Intraoperative video-rate hemodynamic response assessment in human cortex using snapshot hyperspectral optical imaging. Neuophotonics 3, 045003.

Pieczywek, P.M., Cybulska, J., Szymanska-Chargot, M., Siedliska, A., Zdunek, A., Nobalewicz, A., Baranowski, P., Kurenda, A., 2018. Early detection of fungal infection of stored apple fruit with optical sensors – comparison of biospeckle, hyperspectral imaging and chlorophyll fluorescence. Food Control 85, 327-338.

Pietikainen, M., Hadid, A., Zhao, G., Anonen, T., 2011. Computer vision using local binary patterns. Springer, London, UK.

Plaza, A., Plaza, J., 2011. Parallel Hyperspectral Image and Signal Processing IEEE Signal Processing Magazine 28, 119 - 126

Polder, G., van der Heijden, G.W.A.M., van der Voet, H., Young, I.T., 2004. Measuring surface distribution of carotenes and chlorophyll in ripening tomatoes using imaging spectrometry. Postharvest Biology and Technology 34, 117-129.

Pudil, P., Novovicova, J., Kittler, J., 1994. Floating search methods in feature selection. Pattern Recognition Letters 15, 1119-1125.

Qin, J., 2010. Hyperspectral imaging instruments, In: Sun, D.W. (Ed.), Hyperspectral imaging for food quality analysis and control. Academic Press, London, UK, pp. 129-172.

Qin, J., Burks, T.F., Kim, M.S., Chao, K., Ritenour, M.A., 2008. Citrus canker detection using hyperspectral reflectance imaging and PCA-based image classification method. Sensing and Instrumentation for Food Quality and Safety 2, 168-177.

Qin, J., Burks, T.F., Ritenour, M.A., Bonn, W.G., 2009a. Detection of citrus canker using hyperspectral reflectance imaging with spectral information divergence. Journal of Food Engineering 93, 183-191.

Qin, J., Burks, T.F., Zhao, X., Niphadkar, N., Ritenour, M.A., 2011a. Multispectral detection of citrus canker using hyperspectral band selection. Transactions of the ASABE 54, 2331-2341.

Qin, J., Chao, K., Kim, M.S., 2010. Raman chemical imaging system for food safety and quality inspection. Transactions of the ASABE 53, 1873-1882.

Qin, J., Chao, K., Kim, M.S., 2011b. Investigation of Raman chemical imaging for detection of lycopene changes in tomatoes during postharvest ripening. Journal of Food Engineering 107, 277-288.

Qin, J., Chao, K., Kim, M.S., 2016. Raman scattering for food quality and safety assessment, In: Lu, R. (Ed.), Light scattering technology for food property, qualty and safety assessment. CRC Press, Bota Raton, FL, USA, pp. 387-428.

Qin, J., Kim, M.S., Chao, K., Chan, D.E., Delwiche, S.R., Cho, B.K., 2017a. Line-scan hyperspectral imaging techniques for food safety and quaity applications. Applied Sciences 7, 125.

Qin, J., Kim, M.S., Chao, K., Schmidt, W.F., Cho, B.K., Delwiche, S.R., 2017b. Line-scan Raman imaging and spectroscopy platform for surface and subsurface evaluation of food safety and quality. Journal of Food Engineering 198, 17-27.

Qin, J., Lu, R., 2005. Detection of pits in tart cherries by hyperspectral transmission imaging. Transactions of the ASAE 48, 1963-1970.

Qin, J., Lu, R., 2008. Measurement of the optical properties of fruits and vegetables using spatially resolved hyperspectral diffuse reflectance imaging technique. Postharvest Biology and Technology 49, 355-365.

Qin J., Lu, R., Peng, Y., 2009b. Prediction of apple internal quality using spectral absorption and scattering properties. Transactions of the ASABE 52, 499-507.

Rady, A., Ekramirad, N., Adedeji, A.A., Li, M., Alimardani, R., 2017. Hyperspectral imaging for detection of codling moth infestation in GoldRush apples. Postharvest Biology and Technology 129, 37-44.

Rajkumar, P., Wang, N., ElMasry, G., Raghavan, G.S.V., Gariepy, Y., 2012. Studies on banana fruit quality and maturity stages using hyperspectral imaging. Journal of Food Engineering 108, 194-200.

Ramponi, G., Strobel, N., Mitra, S.K., Yu, T.H., 1996. Nonlinear unsharp masking methods for image contrast enhancement. Journal of Electronic Imaging 5, 353-366.

Reid, M.S., 2002. Maturation and maturity indices, In: Kader, A.A. (Ed.), Postharvest quality of horticultural crops. Univ of California Agriculture & Natural Resources, pp. 55-62.

Rungpichayapichet, P., Nagle, M., Yuwanbun, P., Khuwijitjaru, P., Mahayothee, B., Muller, J., 2017. Prediction mapping of physicochemical properties in mango by hyperspectral imaging. Biosystems Engineering 159, 109-120.

Saeys, W., Do Trong, N.N., Van Beers, R., Nicolai, B.M., 2019. Multivariate calibration of spectroscopic sensors for postharvest quality evaluation: A review. Postharvest Biology and Technology 158, 110981.

Saeys, Y., Inza, I., Larrañaga, P., 2007. A review of feature selection technqiues in bioinformatics. Bioinformatics 23, 2507-2517.

Saranwong, S., Haff, R.P., Thanapase, W., Janhiran, A., Kasemsumran, S., Kawano, S., 2011. A feasibility study using simplified near infrared imaging to detect fruit fly larvae in intact fruit. Journal of Near Infrared Spectroscopy 19, 55-60.

Sarkar, N., Wolfe, R.R., 1985. Computer vision based system for quality separation of fresh market tomatoes. Transactions of the ASAE 28, 1714-1718.

Scholkopf, B., Smola, A.J., 2002. Learning with kernels: support vector machines, regularization, optimization, and beyond. The MIT Press, Cambridge, MA, USA.

Shearer, S.A., Payne, F.A., 1990. Color and defect sorting of bell peppers using machine vision. Transactions of the ASAE 33, 2045–2050.

Siedliska, A., Baranowski, P., Zubik, M., Mazurek, W., 2017. Detection of pits in fresh and frozen cherries using a hyperspectral system in transmittance mode. Journal of Food Engineering 215, 61-71.

Siripatrawan, U., Makino, Y., Kawagoe, Y., Oshita, S., 2011. Rapid detection of Escherichia coli contamination in packaged fresh spinach using hyperspectral imaging. Talanta 85, 276-281.

Slaughter, D.C., Obenland, D.M., Thompson, J.F., Arpaia, M.L., Margosan, D.A., 2008. Non-destructive freeze damage detection in oranges using machine vision and ultraviolet fluorescence. Postharvest Biology and Technology 48, 341-346.

Song, D., Song, L., Sun, Y., Hu, P., Tu, K., Pan, L., Yang, H., Huang, M., 2016. Black heart detection in white radish by hyperspectral transmittance imaging combined with chemometric analysis and a successive projections algorithm. Applied Sciences 6, 249.

Sonka, M., Hlavac, V., Boyle, R., 2015. Image processing, analysis, and machine vision. Cengage Learning, Stamford, CT, USA.

Sze, V., Chen, Y.H., Yang, T.J., Emer, J.S., 2017. Efficient processing of deep neural networks: a tutorial and survey. Proceedings of the IEEE 105, 2295-2329.

Szeliski, R., 2011. Computer vision: algorithms and applications. Springer, London, UK.

Taghizadeh, M., Gowen, A., Ward, P., O'Donnell, C. P., 2010. Use of hyperspectral imaging for evaluation of the shelf-life of fresh white button mushrooms (*Agaricus bisporus*) stored in different packaging films. Innovative Food Science & Emerging Technologies 11, 423-431.

Tallada, J.G., Nagata, M., Kobayashi, T., 2006. Non-destructive estimation of firmness of strawberries (*Fragaria×ananassa Duch*.) using NIR hyperspectral imaging. Environmental Control in Biology 44, 245-255.

Throop, J.A., Aneshansley, D.J., Upchurch, B.L., 1993. Near-IR and color imaging for bruise detection on Golden Delicious apples, Proceedings Volume 1836, Optics in Agriculture and Forestry. SPIE, pp. 33-44.

Unay, D., Gosselin, B, 2007. Stem and calyx recognition on 'Jonagold' apples by pattern recognition. Journal of Food Engineering 78, 597-605.

van der Maatten, L., Postma, E., van den Herik, J., 2009. Dimensionality reduction: a comparative review. Tilburg University.

Vanoli, M., Van Beers, R., Sadar, N., Rizzolo, A., Buccheria, M., Grassia, M., Lovatia, F., Nicolaï, B., Aernouts, B., Watté, R., Torricelli, A., Spinelli, L., Saeys, W., Zanella, A., 2020. Time- and spatially-resolved spectroscopy to determine the bulk optical properties of ‘Braeburn’ apples after ripening in shelf life. Postharvest Biology and Technology, 168, 111233. doi: 10.1016/j.postharvbio.2020.111233

van Roy, J., Keresztes, J.C., Wouters, N., De Ketelaere, B., Saeys, W., 2017. Measuring colour of vine tomatoes using hyperspectral imaging. Postharvest Biology and Technology 129, 79-89.

Vargas, A.M., Kim, M.S., Tao, Y., Lefcourt, A.M., Chen, Y.R., Luo, Y., Song, Y., Buchanan, R., 2005. Detection of fecal contamination on cantaloupes using hyperspectral fluorescence imagery. Journal of Food Science 70, 471-476.

Varmuza, K., Filzmoser, P., 2009. Introduction to multivariate Statistical Analysis in chemometrics. CRC Press, Boca Raton, FL, USA.

Wang, H., Li, C., Wang, M., 2013. Quantitative determination of onion internal quality using reflectance, interactance, and transmittance modes of hyperspectral imaging. Transactions of the ASABE 56, 1623-1635.

Wang, J.N., K., Ohashi, S., Kubota, Y., Takizawa, K., Sasaki, Y., 2011. Detection of external insect infestations in jujube fruit using hyperspectral reflectance imaging. Biosystems Engineering 108, 345-351.

Wang, Z., Van Beers, R., Aernouts, B., Watté, R., Verboven, P., Nicolai, B., Saeys, W., 2020. Microstructure affects light scattering in apples. Postharvest Biology and Technology, 159, 110996. doi: 10.1016/j.postharvbio.2019.110996

Wendel, A., Underwood J., Walsh, J., 2018. Maturity estimation of mangoes using hyperspectral imaging from a ground based mobile platform. Computers and Electronics in Agriculture 155, 298-313.

Westerhuis, J.A., de Jong, S., Smilde, A.K., 2001. Direct orthogonal signal correction. Chemometrics and Intelligent Laboratory Systems 56, 13-25.

Wold, S., Antti, H., Lindgren, F., Ohman, J., 1998. Orthogonal signal correction of near-infrared spectra. . Chemometrics and Intelligent Laboratory Systems 44, 175-185.

Wu, H., Haibach, F.G., Bergles, E., Qian, J., Zhang, C., Yang, W., 2014. Miniaturized handheld hyperspectral imager, In: Druy, M.A., Crocombe, R.A. (Eds.), Next-Generation Spectroscopic Technologies VII. SPIE, Baltimore, MD, USA.

Xing, J., Bravo, C., Jancsok, P.T., Ramon, H., De Baerdemaeker, J., 2005. Detecting bruises on 'Golden Delicious' apples using hyperspectral imaging with multiple wavebands. Biosystems Engineering 90, 27-36.

Xing, J., De Baerdemaeker, J., 2005. Bruise detection on 'Jonagold' apples using hyperspectral imaging. Postharvest Biology and Technology 37, 152-162.

Xing, J., Saeys, W., De Baerdemaeker, J., 2007. Combination of chemometric tools and image processing for bruise detection on apples. Computers and electronics in agriculture, 56, 1-13.

Xing, J., Guyer, D., Ariana, D., Lu, R., 2008. Determining optimal wavebands using genetic algorithm for detection of internal insect infestation in tart cherry. Sensing and Instrumentation for Food Quality and Safety 2, 161-167.

Yang, C., Lee, W.S., Gader, P., 2014. Hyperspectral band selection for detecting different blueberry fruit maturity stages. Computers and Electronics in Agriculture 109, 23-31.

Yang, C.C., Chao, K., Kim, M.S., 2009. Machine vision system for online inspection of freshly slaughtered chickens. Sensing and Instrumentation for Food Quality and Safety 3, 70-80.

Yang, C.C., Kim, M.S., Kang, S., Tao, T., Chao, K., Lefcourt, A.M., Chan, D.E., 2011. The development of a simple multispectral algorithm for detection of fecal contamination on apples using a hyperspectral line-scan imaging system. Sensing and Instrumentation for Food Quality and Safety 5, 10-18.

Yang, W., Wang, K., Zuo, W., 2012. Neighborhood component feature selection for high-dimensional data. Journal of Computers 7, 161-167.

Yoon, S.C., Park, B., Lawrence, K.C., Windham, W.R., Heitschmidt, G.W., 2011. Line-scan hyperspectral imaging sytem for real-time inspection of poultry carcasses with fecal material and ingesta. Computers and Electronics in Agriculture 79, 159-168.

Yu, X., Lu, H., Wu, D., 2018. Development of deep learning method for predicting firmness and soluble solid content of postharvest Korla fragrant pear using Vis/NIR hyperspectral reflectance imaging. Postharvest Biology and Technology 141, 39-49.

Yue, J., Yang, G., Li, C., Li, Z., Wang, Y., Feng, H., Xu, B., 2017. Estimation of winter wheat above-ground biomass using unmanned aerial vehicle-based snapshot hyperspectral sensor and crop height improved models. Remote Sensing 9, 708.

Zhang, B., Li, J., Fan, S., Huang, W., Zhao, C., Liu, C., Huang, D., 2015a. Hyperspectral imaging combined with multivariate analysis and band math for detection of common defects on peaches (Prunus persica). Computers and Electronics in Agriculture 114, 14-24.

Zhang, B., Li, J., Huang, W., Fan, S., Zhao, C., Meng, Q., 2015b. Development of a hyperspectral imaging system for the early detection of apple rottenness caused by *Penicillium*. Journal of Food Process Engineering 38, 499-509.

Zhang, M., Jiang, Y., Li, C., Yang, F., 2020. Fully convolutional networks for blueberry bruising and calyx segmentation using hyperspectral transmittance imaging. Biosystems Engineering 192, 159-175.

Zhang, M., Li, C., Takeda, F., Yang, F., 2017. Detection of internally bruised blueberries using hyperspectral transmittance imaging. Transactions of the ASABE 60, 1489-1502.

Zhang, R.Y., Y., Rao, X., Li, J., 2012. Quality and safety assessment of food and agricultural products by hyperspectral fluorescence imaging. Journal of the Science of Food and Agriculture 92, 2397-2408.